THE JOURNAL OF PHYSICAL CHEMISTRY C
A JOURNAL OF THE AMERICAN CHEMICAL SOCIETY

pubs.acs.org/JPCC

Article

Enlighted: Silver Nanoparticles Undergo Photoinduced Shape Transformations and Are Photostable When Coated with Hybrid Lipid Membranes

Citlali Nieves Lira, Marilyn R. Mackiewicz,* and Hao Yue

Cite This: *J. Phys. Chem. C* 2024, 128, 21784−21799

Read Online

ACCESS | Metrics & More | Article Recommendations | Supporting Information

ABSTRACT: Producing silver nanoparticles (AgNPs) of homogeneous shapes and sizes that are stable for oxidation remains challenging. Here, a fast and accessible synthesis is presented to tune the homogeneity of triangular plates (AgNPLs) using light. This study showed AgNPs of varying shapes (spheres, rounded triangles, and rods), sizes (10−20, 40, and 33 nm, respectively), and surface chemistry (citrate and PVP capping agents) undergo a light-induced conversion to 75−85% sharp AgNPLs with a narrow-localized surface plasmon resonance (LSPR) band with λ_{max} at 680 nm and an average edge length of 40 nm ± 5.6 nm as confirmed by UV−vis spectroscopy and transmission electron microscopy (TEM), respectively. Further exploration into the mechanism confirmed that Ag^+ ions, O_2, and light are critical parameters for the light-induced transformation of AgNSs to AgNPLs. Under an inert atmosphere, shape transformation is inhibited, reinforcing the essential role of O_2 in the process. More remarkably, when AgNPs of any size or shape are coated with a hybrid lipid-coated membrane, the AgNPs had exceptional photostability, showing no change LSPR band, underscoring their resistance to photooxidation and shape transformation even in the presence of excess Ag^+ ions, O_2, and AgNSs. The results highlight the importance of light in tuning the homogeneity of AgNPs and the superior stabilizing effect of hybrid lipid membranes.

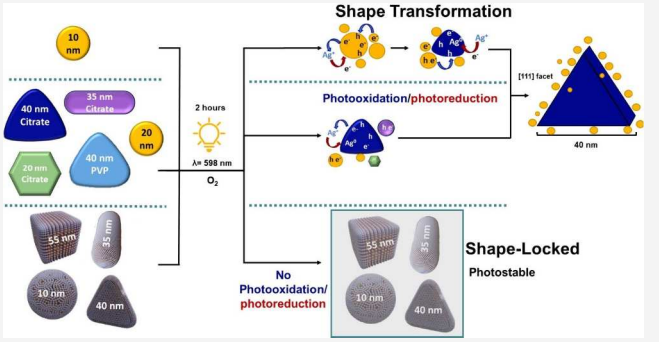

INTRODUCTION

By harnessing the remarkable optical, chemical, physical, biological, catalytic, and antimicrobial properties,[1−3] silver nanoparticles (AgNPs) have made their mark in emerging commercialized markets and are used in various industrial and biomedical applications. Over the past decade, this potential for diverse applications has inspired chemists to optimize reaction conditions and synthetic methods to produce AgNPs with finely tuned homogeneity. Their physicochemical parameters (size, shape, surface charge) directly influence their intrinsic properties, such as the localized surface plasmon resonance band (LSPR), surface-enhanced Raman scattering (SERS), metal-enhanced fluorescence, and catalytic activity.[4−8] The homogeneity and physicochemical characteristics of the AgNPs are critical factors for ensuring consistency. These properties directly impact the material's performance in various applications, particularly in medicine, where precise dosing is essential for optimal efficacy and safety.[9−11] Moreover, the physicochemical properties of nanoparticles play a pivotal role in influencing their effectiveness and interactions with biological systems, which in turn influence uptake and retention.[12−14] Understanding and manipulating these properties is crucial in developing effective and safe nanomaterials. In addition, while several synthetic procedures exist for producing AgNPs, they do not fully capture all shapes and sizes and few procedures still exist to control their homogeneity and physicochemical properties. There is also still a need for environmentally friendly, low-cost, practical synthetic approaches to producing homogeneous AgNPs.[15] Their propensity to undergo surface oxidation and release Ag^+ ions also underscores the difficulty of producing high-quality AgNPs with consistent homogeneity, physicochemical properties, and improved stability.

Chemists have developed several methods for tuning the physicochemical properties and homogeneity of spheres,[5] rods,[16−19] cubes,[4,8,20−22] triangular nanoplates[6,23−28] or nanoprisms, triangular bipyramids[25] and nanodisks[29] with a wide variety of capping agents. The two predominant methods include a chemical method, a two-step process, where AgNP seeds (4−10 nm) are formed by chemically reducing metals in the presence of stabilizing agents.[6,23−28,30−32] These seeds are

Received: September 3, 2024
Revised: November 13, 2024
Accepted: December 3, 2024
Published: December 12, 2024

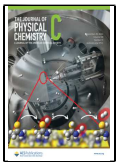

grown into isotropic or anisotropic shapes by adding further reducing agents and metal ions.[18,33−35] The second method is a photochemical approach that generates several distinct shapes from AgNP seeds and is mainly used to synthesize AgNPLs or nanoprisms.[16,25,26,36,37] Various light sources have been used to excite the reaction system, such as laser lines,[38] light-emitting diodes (LEDs),[39−41] UV lamps, Xenon,[34] and sodium lamps.[4−8] Besides having a higher degree of control over the size and shape of the AgNPs, the photochemical approach is eco-friendly, sustainable, low cost, and lacks hazardous byproducts compared to the chemical method. Whereas in the chemical methods, cetyltrimethylammonium bromide (CTAB) or cetyltrimethylammonium cations (CTA) are used to tune the physicochemical features of the AgNPs, which, if not removed, can be toxic.[15,42] Although each method has its advantages and disadvantages, addressing the challenges associated with tuning the physicochemical features and homogeneity is crucial. These methods have undeniably yielded substantial insights into nanoparticle growth and shape transformation mechanisms.

In various study designs, distinct mechanisms have been suggested for nanoparticle growth and shape transformation using chemical and photochemical approaches. The chemical transformation of spherical silver nanoparticles (AgNSs) seeds into nanoprisms has been proposed to occur through seed coalescence and dissolution-recrystallization mechanisms.[43] Extensive mechanistic studies by Schatz, Mirkin, and others show that photomediated nanocrystal growth and shape transformation of AgNP seeds is a complex interplay between light, reactants, and kinetics.[16,25,44−46] The reducing agent, citrate, and a shape-directing surfactant is necessary for the transformation of AgNS seeds to nanoprisms[45] and high pH is required for formation of stable triangular bipyriamids.[25] Citrate also serves as a protective layer on the AgNP [111]-type facets, fills hot charge carrier vacancies on the surface, and acts as a sacrificial electron donor to degrade into acetoacetate.[6,23−28,43] O_2 is also required for the transformation of AgNP seeds into nanoprisms, which oxidizes smaller Ag^0 nanoparticles (2−6 nm) to produce a source of Ag^+ ions, whose solubility increases in the presence of ligands such as Bis(*p*-sulfonatophenyl)phenylphosphine dihydrate dipotassium (BSPP).[44] In addition, the size of the nanoprisms increases linearly with the excitation wavelength, which shows that light is also a critical parameter for the photodevelopment process.[44,45,47,48] Here, plasmon excitation leads to a charge transfer process between adsorbates and the hot electrons (holes) that are produced from plasmon decay.[30−32] In the presence of light, AgNPs serve as photocatalysts to reduce soluble BSPP-Ag^+ at their crystalline faces, where ligand dissociation also occurs.[44] Bach *et al.* show that the excitation wavelength and photon flux strongly influence the reaction dynamics during the photodevelopment of nanoprisms from AgNP seeds and the photoablation of nanoprisms to disks.[46] The shorter the wavelength, the faster the reaction kinetics for nanoprism formation and *vice versa*.[46] Bach *et al.* also showed that nanoprism growth is a light-activated two-dimensional coalescence mechanism. Ostwald ripening becomes the dominant reaction mechanism when larger Ag nanoprisms are grown from photochemically synthesized smaller nanoprisms.[46] Furthermore, the sizes of the original seeds and photon flux are critical parameters that determine the quality of the nanoprism solutions.[46] These foundation studies have offered valuable insight into classical light-driven AgNP growth and shape transformation mechanisms. The impact of light, reaction starting materials, and various capping ligands on the transformation rate and homogeneity of AgNPs has not been sufficiently investigated. Indeed, the variety of lamp sources used in previous studies has shown some contrasting results. In addition, strategies that prevent photomediated redox cycling to improve long-term stability and homogeneity remain challenging.

In this study, UV−vis spectroscopy and transmission electron microscopy (TEM) were used to rigorously evaluate the impact of light on tuning the homogeneity of AgNPs when the starting source is spherical AgNP seeds, AgNPs comprised of a heterogeneous mixture, and AgNPs derived from nonspherical shapes. We examined the effect of a hybrid lipid-coating on shielding the AgNP surface from oxidation and shape transformation in the presence of light. The impact of Ag^+ ions, AgNP seeds, O_2, and capping ligands on the redox chemistry for tuning the physicochemical properties and homogeneity of AgNPs is also examined with citrate-coated, PVP-coated, and hybrid lipid-membrane-coated AgNPs. Our studies have unequivocally advanced our understanding of the classical mechanisms involved in photomediated AgNP growth, shape transformation, and ablation, which have implications for methods that allow us to improve the reproducibility of homogeneous AgNPs and strategy for producing photostable AgNPs.

EXPERIMENTAL METHODS

Reagents. Chemically synthesized and commercially available AgNPs of varying sizes and shapes were used in this study. Aqueous solutions of citrate-capped 20 nm AgNSs, 100 nm of PVP-capped silver AgNPLs, and 100 nm of PVP-capped−silver nanocubes (AgNCs) were purchased from Nanocomposix.com (San Diego, CA, USA). TWEEN 20, Chloroform ($CHCl_3$), 95% 1-hexanethiol (HT), sodium oleate (SOA), sodium borohydride ($NaBH_4$), sodium hydroxide (NaOH), trisodium citrate ($Na_3C_6H_3O_7$), and L-α-phosphatidylcholine (PC) was purchased from Sigma-Aldrich, while potassium cyanide (KCN) was from Mallinckrodt. Silver nitrate ($AgNO_3$) was from G. Frederick Smith Chemical Co. All reagents were used as received. Sodium phosphate monobasic monohydrate and sodium phosphate dibasic heptahydrate were from BDH Chemicals. Ultracentrifugation was performed with Thermo Scientific Sorvall ST 40R Vivaspin concentrators with PES membranes with a molecular weight cuff off (MWCO) of 10 kDa from Thermofisher Scientific, Hillsboro, OR, USA.

Preparation of Citrate-capped AgNS, AgNPLs, and AgNRs. Using a modified procedure,[49,50] $AgNO_3$ (43 mL of 0.109 mM in H_2O) was combined with H_2O_2 (120 μL of 30% w/w) and $Na_3C_6H_3O_7$ (3.68 mL of 34.2 mM in H_2O) in a 250 mL Erlenmeyer flask, which was covered with aluminum foil to protect the solution from light exposure. The mixture was allowed to stir at 600 rpm with a medium-sized stir bar for 2 min before a freshly prepared aqueous solution of $NaBH_4$ (220 μL of 110 mM in H_2O) was rapidly added to the center of the reaction vortex in the flask. Note: $NaBH_4$ is weighed out right before dissolution and added to the sample to ensure minimal decomposition of the reducing agent. Rapid addition of $NaBH_4$ to the solution resulted in a fast color change for approximately 2−3 min, changing from pale yellow to orange to purple and, finally, a navy-blue color indicative of AgNPLs. For AgNSs, 880 μL of 110 mM of freshly prepared $NaBH_4$ in H_2O was

https://doi.org/10.1021/acs.jpcc.4c05948
J. Phys. Chem. C 2024, 128, 21784−21799

rapidly added to the reaction vortex, which resulted in a deep amber-yellow solution, indicative of AgNSs. AgNSs and AgNPLs were stirred for an additional 20 min before being covered and stored in the refrigerator at 4 °C overnight. For AgNRs, 215 μL of 0.2 M of freshly prepared $NaBH_4$ in H_2O was rapidly added to 2 mL of AgNSs with λ_{max} 401 nm with an O.D. of 1.0. The sample was exposed to a 300 W xenon lamp with a 420 nm bandpass filter for 2 h to achieve a light purple solution characteristic of AgNRs. UV−vis spectra were recorded in triplicate for all samples.

Fine-tuning the Homogeneity of AgNPs Using a 70-W Sodium Lamp. In a 5 mL vial, 2 mL of citrate-capped AgNSs (O.D. of 1.2), PVP-capped AgNPLs (O.D. of 1.3), AgNCs (O.D. of 2.6), or AgNRs (O.D. of 1.1), were irradiated separately using a Plusrite 70 W high-pressure sodium lamp with an emission spectrum ranging from 570 to 650 nm with strong peaks in the yellow-orange region for 2 h that was housed in a foiled-wrapped box (Figure S1). The resulting solution changed from yellow (AgNSs), light blue (AgNPLs), or light purple (AgNRs) to a deep navy-blue solution after light exposure. UV−vis spectra were recorded in triplicate for all samples.

Preparation of Hybrid Lipid-Coated AgNPs. Using an established procedure,[50−53] SOA (1.1 μL of 9.4 mM in H_2O) was added to 10 nm citrate-capped AgNS (1 mL of AgNSs at O.D 1.2 and λ_{max} 410 nm in H_2O). The solution was left to stir for 20 min at 600 rpm to form Ag-SOA. This was followed by adding PC liposomes (10.4 μL of 0.54 mM in 10 mM sodium phosphate buffer (PB) at pH 8.0) and was incubated for 40 min to form Ag-SOA-PC. The PC liposome was prepared by evaporating a PC solution (1 mL of 3.3 mM of PC in $CHCl_3$) under a stream of N_2 to form a thin film that was dried under vacuum for 12 h. The film was resuspended with 2 mL of 10 mM PB at pH 8, shaken vigorously by hand, and sonicated for 90 min in 15 °C water until clear. To Ag-SOA-PC, a room-temperature solution of HT was added (1.4 μL of 30 mM solution in ethanol), which was incubated for a minimum 30 min. The resulting Ag-SOA-PC-HT was purified by incubating the sample with 10 μL of Tween20 (10 mM in H_2O) for every mL of Ag-SOA-PC-HT for 1 h before ultracentrifugation at 4700 rpm using a Vivaspin 20 column with a 10 kDa PES membrane. The sample was washed with 10 mL of 10 mM PB buffer seven times. The same method was followed for silver nanocubes (AgNCs), AgNPLs, and silver nanorods (AgNRs), with volume alterations to cover the nanoparticle's surface (Table S1) completely. A well-known cyanide etch test is performed to determine if the hybrid lipid membrane coating entirely covered the AgNPs.[54] Briefly, 1.0 mL of Ag-SOA-PC-HT (1.0 O.D.) was exposed to 20 μL of 307 mM of KCN for a final concentration of 6.14 mM KCN for 1 h. The UV−vis spectrum was taken for all samples described here, where the percent change in the λ_{max} and O.D. was monitored to assess AgNP stability. Each batch of hybrid lipid-coated AgNPs was tested for cyanide stability (Figure S2).

Mechanistic Studies. The following samples were prepared to study the effect of AgNPs, Ag^+ ions, and O_2 on photoinduced shape transformation. To evaluate the role of Ag^+ ions on shape transformation, 200 μL of 110 mM $AgNO_3$ (aq) solution was added to each 2 mL sample of chemically synthesized 10 nm citrate-capped AgNSs with an O.D. of 1.3 or 10 nm hybrid lipid-coated AgNSs with an O.D. of 1.5 to yield a final concentration of 10 mM of $AgNO_3$. To examine the role of chemically AgNSs on shape transformation, 200 μL of chemically synthesized 10 nm citrate-capped AgNSs with an O.D. of 0.19 was added to 40 nm commercially purchased PVP-capped AgNPLs with an O.D. of 0.27 with a λ_{max} of 620 nm. To determine the effect of hybrid lipid-coated AgNPs on shape transformation, 200 μL of 10 nm hybrid lipid-coated AgNSs with an O.D. of 0.32 were added to 2 mL of 40 nm purchased PVP-capped AgNPLs with an O.D. of 0.41. To evaluate the role of O_2 in the reaction, 100 μL of chemically synthesized 10 nm citrate-capped AgNSs with an O.D. of 1.12 were placed in a 20 mL vial, capped with a septum and degassed with N_2 for 5 min. Lastly, to examine the role of Ag^+ ions in the presence and absence of O_2, 2 mL of chemically synthesized 10 nm citrate-capped AgNSs with an O.D. of 1.18 and 2 mL of the same solution spiked with 200 μL of 110 mM $AgNO_3$ (aq) solution with an O.D. of 0.89 were placed in a 20 mL vial, capped with a septum, and degassed with N_2 for 5 min. The degassed N_2 and the control samples with O_2 were placed under the 70-W sodium lamp for 2 h. UV−vis spectra before and after light exposure were recorded. To evaluate the role of citrate and Ag^+ ion in shape transformation, 1.5 mL of commercially purchased 20 nm AgNPs with an O.D. of 0.63 with minimal citrate was incubated with 110 mM $AgNO_3$ or 322 mM trisodium citrate, then exposed to light and then the UV−vis spectra recorded.

^{1}H NMR Studies. The NMR spectra of samples of AgNSs with no light exposure and after light exposure were collected in D_2O. Briefly, 2 mL of the 10 nm citrate-capped AgNSs with an O.D. of 1.1 and a λ_{max} of 401 nm was exposed to the sodium lamp for 2 h. The resulting AgNPL and AgNSs with no light exposure were rotovated separately in vials before resuspension in 1 mL of D_2O for ^{1}H NMR analysis using the Ultrashield Plus 700 MHz NMR Spectrometer.

Physical Measurements. Absorbance measurements were recorded using a Cary 5000 UV−vis-NIR spectrophotometer with a 1.0 cm path length quartz cell cuvette. TEM samples were prepared by drop-casting 5 μL onto carbon-coated (300 Å) Formvar films on copper grids purchased from Ted Pella. The solution was drop-casted on the grid and allowed to dry for 5 min before absorbing the excess sample with filter paper; this process was repeated 3 times. TEM images were acquired on an FEI TITAN 80−200 microscope with a CCD detector at an acceleration voltage of 200 kV. ImageJ software obtained nanoparticle shape and size analysis (Figure S3).

RESULTS AND DISCUSSION

Photochemical Synthesis of Homogenous Citrate-capped AgNPLs. Initially, an established photochemical method was used to produce homogeneous AgNPLs.[7] Briefly, 2 mL of chemically synthesized citrate-capped AgNSs with an LSPR band of λ_{max} of 401 nm and an O.D. of 1.2 (Figure 1A,C) were exposed to 70-W high-pressure sodium lamp operating at a wavelength of 598 nm for 2 h. TEM analysis of the AgNSs shows a homogeneous sample of 90% of 9.5 ± 2.3 nm and 10% of 4.8 ± 0.34 nm AgNPs, 175 NPs were counted, (Figures 1B and C). Upon irradiation of the AgNSs, the internal temperature of the sample peaked at 98 °C in the first 30 min and was constant for the remainder of the exposed time (90 min). Minor condensation is observed at the top of the vial, with a volume decrease of approximately 100 μL consistently lost across all samples after irradiation. The UV−vis spectra of the sample after light exposure for 2 h showed a concomitant rise of two new characteristics LSPR bands, a smaller band at λ_{max} of 480 nm due to oscillation of

https://doi.org/10.1021/acs.jpcc.4c05948
J. Phys. Chem. C 2024, 128, 21784−21799

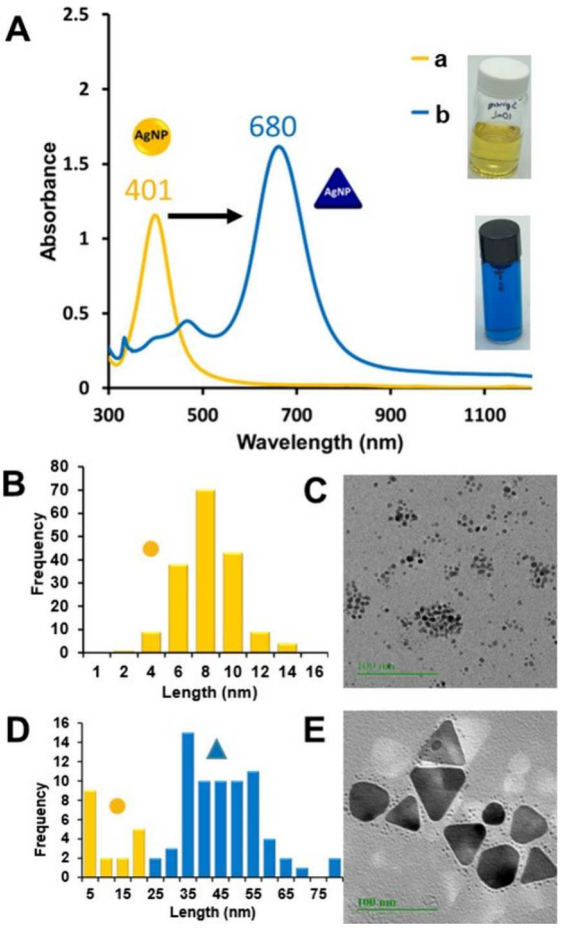

Figure 1. Representative UV−vis spectra of (A) 10 nm citrate-capped AgNSs with an O.D. of 1.2. (a) before light exposure and (b) after light exposure. (B) Histogram of AgNS distribution before light exposure and (C) representative TEM. (D) Histogram of AgNPLs distribution after light exposure and (E) its representative TEM. The scale bar of the TEM is 100 nm.

electrons along the width of the plate and a more intense and sharper near-infrared band at λ_{max} of 680 nm due to oscillations of the electron along the face of the plate. The decrease of the LSPR band at λ_{max} of 401 nm from the AgNSs and consequent red-shift and rise of two new SPR bands indicates the formation of AgNPLs (Figure 1A). TEM analysis of the resulting royal blue solution showed an 85% distribution of AgNPLs (40 nm ±22 nm edge length) and a 15% distribution of spheres (3.0 nm ±0.32 nm), 192 NPs were counted, Figures 1D and E. A description of the AgNP measurements is in Figure S3. Although, Small-angle X-ray scattering (SAXS) analysis in solution was not performed in this study, the shape and intensity of the LSPR band and nanoparticle distribution by TEM is consistent with that observed in other studies where SAXS corroborates the particle distribution observed by TEM and UV−vis.[55,56] The transformation of AgNSs to AgNPLs following light exposure agrees with previous studies where the wavelength produced by the lamp source permits the oxidation of Ag^0 on the AgNP surface to yield a free electron and Ag^+ ion.[57] Since the sample is not under inert conditions and is in the presence of O_2, free or Ag^+ ions produced from the etching of AgNSs may undergo reduction to Ag^0 on the AgNPs surface to yield AgNPLs.[45] This mechanism is supported by the decrease in the LSPR band of AgNSs and TEM analysis showing a reduction in the diameter of the AgNSs from 10 ± 2.3 nm to 3.0 ± 0.34 nm after photolysis (Figure 1). In other studies, nanoparticle growth and shape is typically observed from multiple twinned nanoparticles in the initial stages of growth.[58,59] In this study TEM show no evidence of twinned AgNPs, which suggests the mechanism of growth and shape transformation occurs through a photooxidation route, *vide infra*. The size and shape of the AgNPL and formation rate depend on the length of irradiation time and the lamp's power during this process.[45,60] Longer exposure times of up to 12 h or using a 150-W sodium lamp did not result in 100% conversion of AgNSs to AgNPLs—the heat from the lamp resulted in evaporation of the sample (Figure S4). Under the conditions for this study, a heterogeneous mixture of unconsumed AgNSs (3 nm) and AgNPLs (40 nm edge length) remains after 2 h of light exposure, indicating that the conversion has reached equilibrium under these conditions (Figure 1D and E). While a source of AgNSs is present in the sample, O_2 may be significantly decreased, resulting in an 85% conversion since the vial is capped during photolysis. Adding exogenous Ag^+ ions or O_2 could push the reaction equilibrium to complete conversion of AgNPLs, *via infra*.

The Effect of Heat and Wavelength of Light on AgNPL Formation. To assess the impact of heat on AgNPL conversion in the absence of light, a 2 mL solution of chemically synthesized 10 nm citrate-capped AgNSs with an O.D. 1.2 was covered from light exposure with foil and heated to 98 °C for 2 h. The UV−vis spectra of the resulting solution after 2 h of heating time showed no significant changes in the O.D. or shift in the LSPR band of AgNPs at λ_{max} at 401 nm (Figure 2A) indicating that temperature is not driving shape transformation. That is, light is the primary driver since shape transformation does not occur in the absence of light even when internal solution temperature peaks at 98 °C. However, temperature could indirectly decrease the solubility of oxygen in water, potentially reducing the oxygen available for the photoinduced oxidation of Ag^0 to Ag^+ and rate of shape transformation. To investigate the effect of the wavelength of light on shape transformation, 2 mL solutions of 10 nm citrate-capped AgNSs of 1.3 O.D. and λ_{max} at 401 nm were exposed to 3 different light sources for 2 h, an LED light source of λ_{max} at 500 nm, a xenon lamp at λ_{max} 420 nm, and the sodium lamp at λ_{max} of 598 nm. Overall, the UV−vis spectra shows that all wavelengths of light-induced a photochemical change in the AgNSs as indicated by the change in the O.D. and varying degrees of red-shift in the LSPR band (Figure 2B). Upon exposure to the LED light at 500 nm, the LSPR band of the AgNSs at 401 nm (Figure 2B(a)) decreased slightly and red-shifted by 55 nm to a prominent band at 456 nm with a shoulder at 501 nm (Figure 2B(b)). The color of the solution changed from yellow to pale red, indicating a modification in the size and shape of the nanoparticles. The UV−vis spectra of the AgNSs sample after exposure to a xenon lamp with a wavelength of 420 nm show a significant decrease in the LSPR band at λ_{max} 401 nm and a new red-shifted LSPR band at λ_{max} at 563 nm with a shoulder at 405 nm (Figure 2B(c)). The solution changed from yellow to green with a more significant 162 nm red shift, suggesting the formation of AgNP with a larger size and shape. In this sample, a shoulder at 405 nm suggests remnant AgNSs unconsumed in the light-driven reaction. Compared to the narrow LSPR band of starting AgNSs (Figure 2B(a)), the xenon lamp exposed sample presents a much broader LSPR band, a typical indicator of a

https://doi.org/10.1021/acs.jpcc.4c05948
J. Phys. Chem. C 2024, 128, 21784−21799

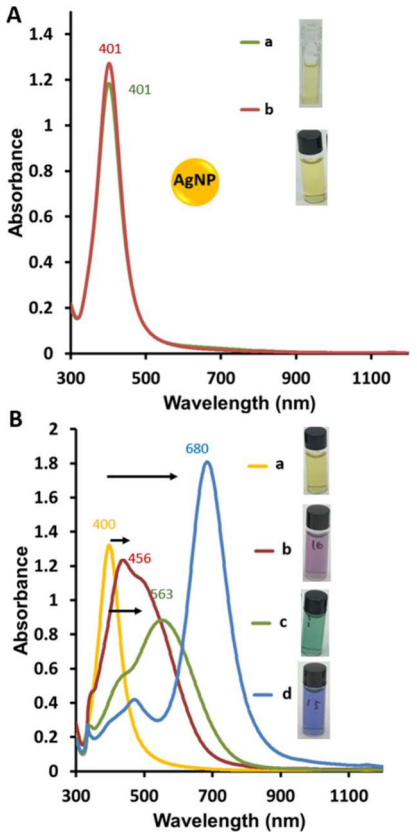

Figure 2. Representative UV−vis spectra of (A) 10 nm citrate-capped AgNSs with an internal solution temperature of 98 °C after 30 min for 2 h in darkness, (a) before heat, and (b) after heat. (B) 10 nm citrate-capped AgNSs (a) before light irradiation and after light irradiation with (b) 500 nm LED light, (c) 420 nm xenon lamp, and (d) 598 nm sodium lamp for 2 h.

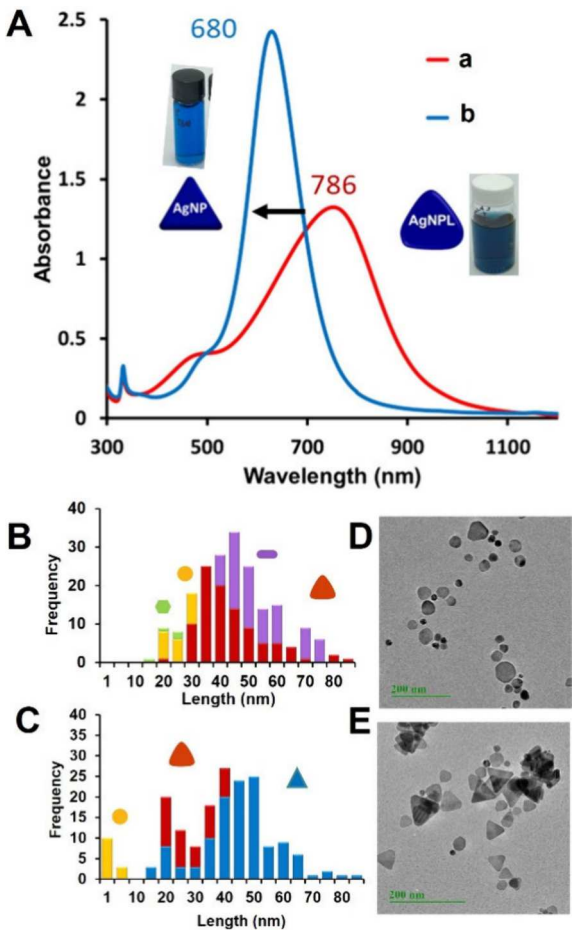

Figure 3. (A) Representative UV−vis spectra of a polydisperse sample of citrate-capped AgNSs, rounded AgNPLs, and AgNRs (a) before light exposure and (b) after light exposure. (B) Histogram of polydisperse AgNPLs distribution before light exposure and (D) representative TEM. (C) Histogram of AgNPLs distribution after light exposure and (E) representative TEM. The scale bar of TEM is 200 nm.

wider distribution of AgNPs of different shapes and sizes (Figure 2B(c)). In contrast, exposure to 598 nm with the sodium lamp showed the typical narrow LSPR band with 279 nm red-shift to λ_{max} at 680 nm with a smaller LSPR band at λ_{max} of 460 nm indicative of AgNPLs and very small shoulder at 400 nm characteristic of AgNSs (Figure 2B(d)). The differences in the observed UV−vis spectra suggest that shape conversion depends on the light source's wavelength and power. This is consistent with studies that show that constant photon flux and varied wavelengths have a pronounced effect on the rate and mechanism of shape transformation.[46]

Photoinduced AgNP Shape Transformation. Studies show that the growth and shape conversion of AgNPs occurs along vertices or edges, which are electron-rich, when exposed to light, transforming one shape of AgNP to another.[57] Consequently, photolysis can be used to tune the homogeneity of AgNPs. To further explore the effect of photolysis and the physicochemical features on shape transformation, various AgNP shapes and heterogeneous populations of AgNPs were exposed to the sodium lamp. Briefly, chemically synthesized citrate-capped AgNPLs were produced following a literature method[49,50] and exposed to the sodium lamp for 2 h. These AgNPLs produced by $NaBH_4$ reduction in the presence of H_2O_2 have two characteristic SPR bands, a small one at λ_{max} of 485 nm and a broad, more intense LSPR band at λ_{max} of 786 nm (Figure 3A). TEM analysis of these AgNPLs shows a polydisperse distribution of 40% of AgNPLs with rounded corners with an edge length of 40 ± 17 nm, 10% of 20 nm ± 6.9 nm AgNSs, and 50% of 48 ± 16 nm in length by 8.9 ± 3.5 nm in width AgNRs, and about 1% of 22 nm ± 1.7 nm hexagons, 200 NPs were counted, (Figure 3B and C). After light exposure, TEM analysis shows a less polydisperse sample comprised of 75% of AgNPLs with sharp edges of 41 ± 15 nm, 15% of 5.0 ± 1.23 nm AgNSs, and 10% rounded AgNPLs with an edge length of 32 ± 10.4 nm, 178 NPs were counted, (Figure 3D and E). The decrease in polydispersity is consistent with the changes observed in the UV−vis spectra that show a blue shift and narrowing of the primary LSPR band at λ_{max} of 786 to 680 nm, respectively (Figure 3A). Although this conversion resulted in a size reduction of the AgNPLs and AgNSs and a narrower distribution, it elucidates an essential contribution to the mechanism that larger citrate-capped AgNPs with a wide variety of shapes can undergo surface oxidation to produce Ag^+ ions that are reduced along vertices or edges of the AgNPs. Given the change in morphology and loss of AgNSs, AgNRs, and rounded AgNPLs, we hypothesize that all shapes undergo conversion to produce more thermodynamically favorable AgNPLs with an absorption band closer in wavelength to the lamp source at 598 nm.

https://doi.org/10.1021/acs.jpcc.4c05948
J. Phys. Chem. C 2024, 128, 21784−21799

In addition to the chemically synthesized polydisperse sample of citrate-capped AgNPLs with rounded corners and AgNSs, a sample primarily composed of citrate-capped AgNRs was exposed to the sodium lamp at 598 nm. Before light exposure, the UV−vis spectra show two characteristic LSPR bands, a shoulder at λ_{max} at 395 nm and a broader and more intense NIR band at λ_{max} at 585 nm. TEM analysis of this sample shows a polydisperse mixture of 60% of 33 ± 8.54 nm in length by 9.7 ± 2.6 nm in width of AgNRs, 20% of rounded AgNPLs with an edge length of 45 ± 8.76 nm, 20% of 19 ± 5.43 nm AgNSs, 222 NPs were counted (Figure 4B and C).

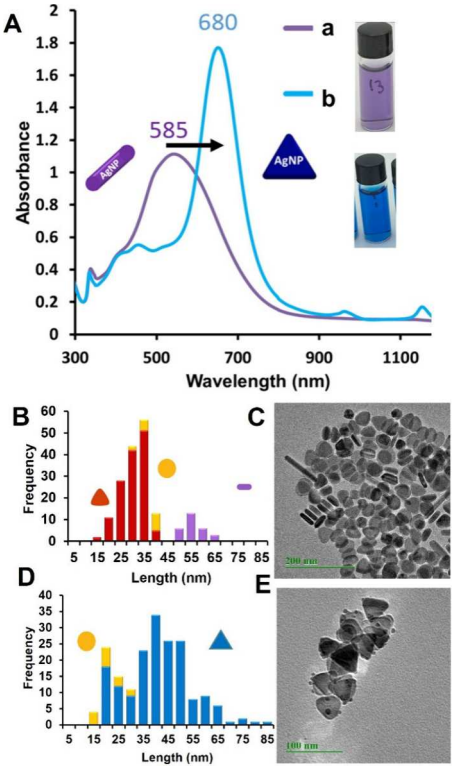

Figure 4. Representative UV−vis of (A) a mixture of predominately citrate-capped AgNRs with AgNSs and AgNPLs, (a) before and (b) after light irradiation. (B) Histogram of nanorods distribution before light exposure and (C) representative TEM. (D) Histogram of nanorods distribution after light exposure and (E) representative TEM. The scale bar is 100 nm.

Upon light irradiation for 2 h under the sodium lamp, the primary broad LSPR band at λ_{max} of 585 nm red-shifted to a narrower LSPR band at λ_{max} of 680 nm, indicative of the AgNPLs (Figure 4A). In addition, a series of smaller bands at 400 and 450 nm, respectively, are also observed. These smaller LSPR bands indicate smaller AgNSs formed from the degradation of AgNSs and AgNRs. TEM analysis of this sample shows that 83% are AgNPLs with sharper edges with an average length of 41.3 ± 13.7 nm and 17% AgNSs with an average diameter of 15 ± 5.3 nm, 192 NPs were counted (Figure 4D and E). TEM images also revealed a significant reduction of other shapes, such as AgNRs and hexagons. Similar to the homogeneous batches of AgNSs (Figure 1), light induces surface oxidation of AgNPs to Ag^+ ions in the presence of O_2 to form AgNPLs at a λ_{max} of 680 nm. The increase in the O.D. and resulting intense solution color suggests photo-induced oxidation of AgNSs and AgNRs followed by the reduction of Ag^+ ions at the surface to form AgNPLs. Similar to 10 nm citrate-capped AgNSs, the small width of the AgNRs (9.7 ± 2.6 nm) also suggests that AgNRs etching occurs from the tip to form AgNSs since no short AgNRs are observed in the TEM after light exposure (Figure 4E). This suggests that the photomorphic transformation of AgNRs to AgNPLs does not occur by coalescence of smaller AgNSs and AgNRs. Instead, the AgNRs undergo surface oxidation at the tips to form AgNSs and Ag^+ ions.

Compared to earlier studies that heavily utilized AgNS seeds,[16,25,26,36,37] the transformation of larger sizes of AgNPs > 10 nm and of AgNRs and hexagons has not been observed. These studies demonstrate that light can be used to tune the optical properties of heterogeneous samples of AgNPs by significantly narrowing their polydispersity. In addition, AgNSs, hexagons, and AgNRs are more suitable for surface oxidation and shape transformation to AgNPLs.

Examining the Influence of Capping Agents on the Photoinitiated Conversion of AgNPs. Literature precedents show that organic stabilizers such as citrate, polyvinylpyrrolidone (PVP),[61] lipids, polyethylene glycol (PEG),[62,63] and thiolated-PEG[64] can stabilize AgNPs to prevent or slow Ag^+ ion release.[62,63] Therefore, to elucidate the effect of the surface ligands on photoinduced transformation, AgNSs, AgNCs, and AgNPLs of varying sizes and shapes capped with different surface ligands intended to prevent rapid surface oxidation were irradiated. Briefly, a sample of the purchased 100 nm PVP-capped AgNPLs with rounded corners with an O.D. of 1.38 and an LSPR band of 980 nm was irradiated for 2 h with the sodium lamp. TEM analysis of the PVP-coated AgNPLs before irradiation comprises a mix of 30% sharp AgNPLs with an edge length of 132 ± 32.1 nm, 50% rounded AgNPLs with an edge length of 47.5 ± 11.6 nm, and 20% 19.64 nm ± 3.85 nm AgNSs, 198 NPs were counted (Figure 5B and C). The UV−vis spectra of the resulting AgNPs showed a significant blue shift from a λ_{max} at 980 to 850 nm and a 21.4% decrease in O.D., indicating a change in size and shape distribution of the purchased 100 nm PVP-capped AgNPLs (Figure 5A). This was confirmed by TEM, which shows a sample comprised of 75% AgNPLs with sharped edges with edge lengths of 43.5 ± 12.7 nm and 25% AgNSs with an average diameter of 15.93 nm ± 4.21 nm, 175 NPs were counted (Figure 5D and E). Although the change was not as dramatic in the UV−vis absorption band as in the 10 nm citrate-capped AgNSs sample (Figure 1), the PVP-coated AgNPL is 50% smaller after irradiation (Figure 5D). In addition, compared to citrate-capped 10 nm AgNSs, which had an 85% conversion to AgNPLs (Figure 1) or the citrate-capped AgNPLs (λ_{max} of 786 nm), which had 75% conversion to sharper AgNPLs (Figure 3A), the 100 nm PVP-coated AgNPLs (λ_{max} of 980 nm) did not undergo the same level of photooxidation and Ag^+ ion release. The decrease in O.D. and lighter color change seen in Figure 5D is consistent with Ag^+ ion oxidation from the surface of the AgNPLs or photoablation. This is evident in the TEM images that show a decrease in size and number of rounded AgNPLs to yield PVP-coated AgNPLs that are smaller with sharper edges at λ_{max} 850 nm as well as a slight increase in the number of AgNSs (Figure 5D and E). In addition, TEM images show that the larger AgNPLs with an edge length of 132 nm have more edges. Hence, these undergo surface oxidation more readily in the presence of a higher energy light source with a wavelength of 598 nm that excites the LSPR at λ_{max} at 950 nm. This is

https://doi.org/10.1021/acs.jpcc.4c05948
J. Phys. Chem. C 2024, 128, 21784−21799

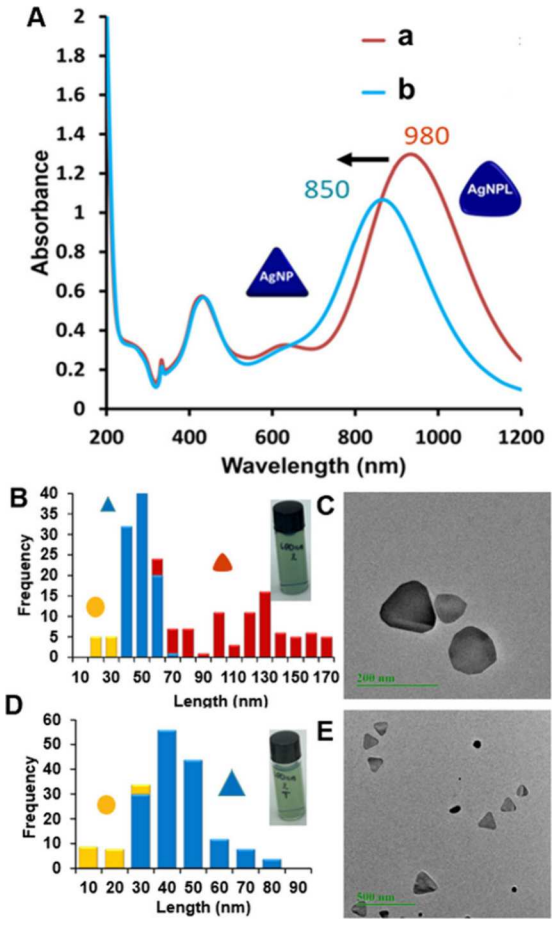

Figure 5. Representative UV−vis of (A) 100 nm PVP-capped AgNPLs (a) before light exposure and (b) after light exposure. (B) Distribution histogram of 100 nm AgNPLs before light exposure and (C) representative TEM. (D) Distribution histogram of nanoplates after light exposure and (E) representative TEM. The TEM scale bar is 500 nm.

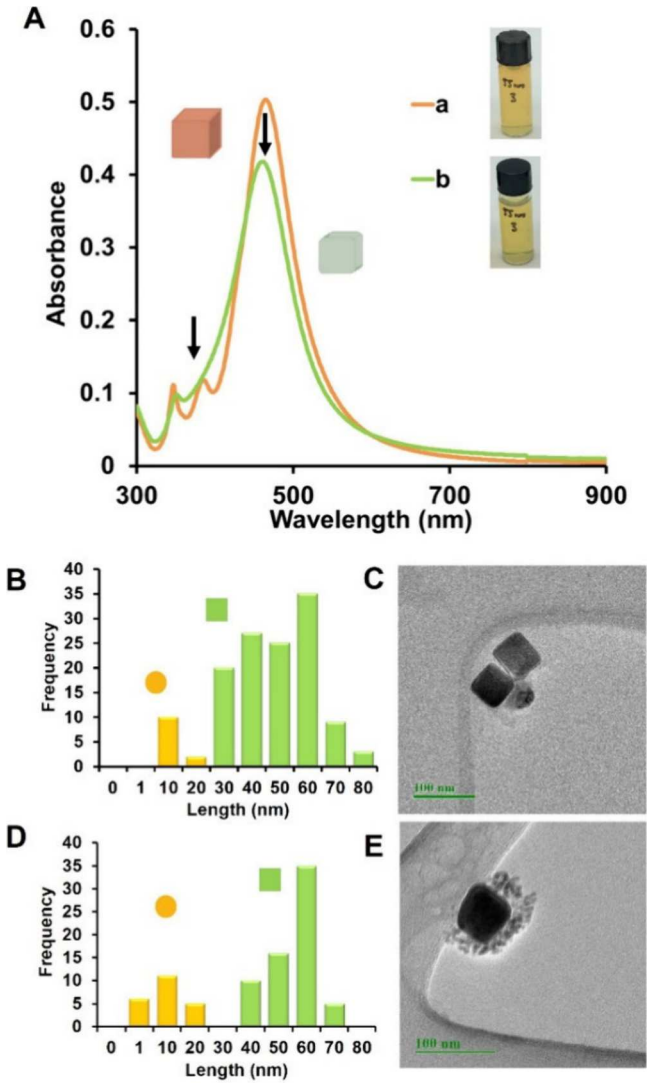

Figure 6. Representative UV−vis of (A) 55 nm PVP-capped AgNCs (a) before and (b) after light exposure for 2 h with a sodium lamp. (B) Histogram of nanocubes distribution before light exposure and (C) representative TEM. (D) Histogram of nanocubes distribution after light exposure and (E) representative TEM. The scale bar is 100 nm.

expected to be the source of Ag^+ ions since the plasmon band at 435 nm, likely due to the AgNSs in the solution, does not change significantly after photolysis in the UV−vis and TEM (Figure 5). The color of the solution is green, indicating the presence of both blue AgNPLs and yellow AgNSs.

Similarly, the UV−vis spectra of PVP-capped AgNCs after irradiation show minimal changes in the LSPR bands (Figure 6). The UV−vis spectra of the PVP-capped AgNCs before irradiation show three narrow LSPR bands at λ_{max} at 368, 400, and 500 nm (Figure 6A). The more intense band at 500 nm is due to electrons' oscillation along the cube's face. TEM analysis of a pale and cloudy yellow solution of purchased 55 nm AgNCs shows a mix of 90% of AgNCs with well-defined edges of 48.5 nm ± 13.1 nm and 10% 10.1 nm ± 2.43 nm AgNSs, 119 NPs were counted (Figure 6B and C). In contrast, unlike the 100 nm PVP-capped AgNPLs, the UV−vis spectra of PVP-capped AgNCs after 2 h of irradiation with the sodium lamp showed a 33.3% decrease in O.D. and 45 nm blue shift of the LSPR band at λ_{max} 500 to 455 nm (Figure 7A), indicating a change size and shape distribution of the PVP-capped AgNCs. TEM analysis confirms the presence of 70% AgNCs with less defined edges with an edge length of 49.2 ± 19.9 nm and 30% of 10.3 ± 1.67 nm AgNSs, 88 NPs were counted. That is, the amount of AgNCs decreases, and the AgNSs increase, which suggests the partial photoinduced transformation of AgNCs to AgNSs. This is evident in the UV−vis spectra, which show the slight growth of the LSPR band at λ_{max} at 400 nm and a decrease in the at λ_{max} at 500 nm. These studies confirm that PVP is a much better stabilizer of AgNPs than citrate, slowing the redox process for AgNP shape transformation. Furthermore, based on the significant changes observed in the UV−vis and TEM, the redox process is slower for PVP-capped AgNCs than AgNPLs, which have higher energy points that are more susceptible to redox chemistry.

Previously, we demonstrated that hybrid lipid membranes can stabilize AgNPs of varying shapes and sizes to prevent surface oxidation over months and enhance their biocompatibility *in vivo*.[50,52,53,65] These hybrid lipid-coated AgNPs are much better for long-term stability than PVP or citrate-capped AgNPs and are stable in the presence of cyanide, a well-known etchant of gold and silver,[66,67] even in the presence of membrane-disrupting surfactants such as sodium dodecyl sulfate, Tween20, and Triton X100.[52] The incredible and

https://doi.org/10.1021/acs.jpcc.4c05948
J. Phys. Chem. C 2024, 128, 21784−21799

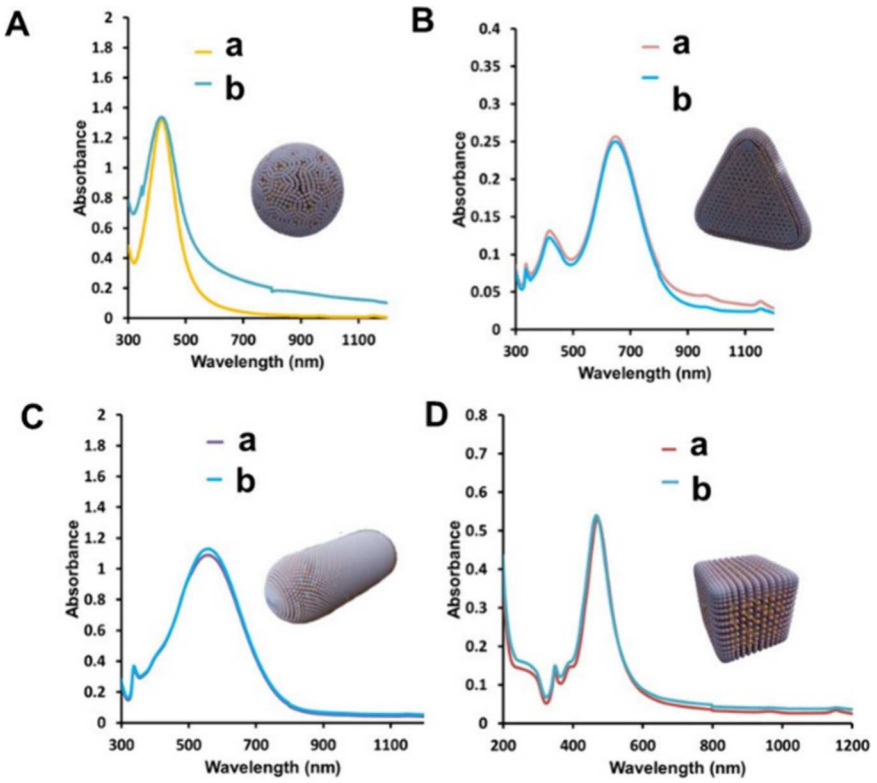

Figure 7. Representative UV−vis of hybrid lipid-coated AgNPs (a) before and (b) after light exposure after 2 h with a sodium lamp: (A) AgNSs, (B) AgNPLs, (C) AgNRs, and (D) AgNCs.

robust AgNP stability results from tight membrane packing from the long chain hydrophobic anchor, hexanethiol or decanethiol, that shields the nanoparticle from surface oxidation in the presence of cyanide. To determine if hybrid lipid coating prevents photooxidation and transformation of the AgNPs, 1 mL samples of hybrid lipid-coated AgNSs, AgNPLs, AgNCs, and AgNRs were exposed to the sodium lamp for 2 h. These samples were prepared by displacing citrate and PVP coatings from the AgNPs using the hybrid lipid membranes. Although the concentration of AgNPs was not the same for each sample, the UV−vis clearly showed no change in O.D. or shift in the LSPR bands, indicating no change in the stability, size, or shape of the hybrid lipid-coated AgNPs (Figure 7). Note the slight increase in the O.D. of the AgNPLs is due to the minor amount of evaporation, which leads to an overall increase in the spectra. The lack of change in the UV−vis spectra and color of the samples indicates no photooxidation to generate Ag^+ ions and no reduction to yield the characteristic AgNPLs at 680 nm. Similar to our prior studies, the hybrid lipid-membrane architecture prevents surface oxidation because it is tightly packed around the AgNP core.[44,50,53,65,68−75] More importantly, it shields the lowest energy [111]-facets where nanoparticle growth is proposed.[44,72−75] This unequivocally demonstrates that light-induced AgNP surface oxidation in the presence of O_2 to generate Ag^+ for reduction at the [111]-facets is critical for nanoparticle growth and shape transformation.[6,16,23−28,44−46] That is, without plasmon excitation and Ag^+ ions near the surface, there is no nanoparticle growth.

The Role of Light, Ag^+ Ions, and AgNSs on Photo-induced Shape Transformation. Literature precedent and these studies herein show that photooxidation of AgNPs to Ag^+ ions followed by reduction to Ag^0 at the surface is necessary for the growth and shape transformation of AgNPs.[44,45] To elucidate further the role of free Ag^+ ions in shape transformation, 200 μL of 110 mM $AgNO_3$ (aq) was added to 2 mL of chemically synthesized 10 nm citrate-capped AgNSs with an O.D of 1.3. No change is observed in the UV−vis spectra upon adding the free Ag^+ ions before irradiation with the same time frame for light exposure (Figure 8A(a)). However, after 120 min of irradiation with the sodium lamp, the yellow citrate-capped AgNS solution changed to blue. The UV−vis spectra showed a 100% decrease in the LSPR band at λ_{max} of 400 nm and the concomitant growth of the LSPR band with λ_{max} of 680 nm, characteristic of AgNPLs (Figure 8A(b)). This is consistent with prior studies showing that light and Ag^+ ions are necessary for their deposition and reduction at the surface, which only occurs after photoexcitation of the LSPR band induces localized ligand dissociation.[44,76−78] In this case, the Ag^+ ion sources come from the exogenous $AgNO_3$ and AgNS seeds, which undergo oxidation and dissolution, as evident from the 100% decrease in the LSPR band at 400 nm (Figure 8A(b)). Similarly, when 100 μL of chemically synthesized 10 nm citrate-capped AgNSs with a λ_{max} of 400 nm and O.D. of 0.8 is added to 1 mL of commercially purchased 40 nm PVP-capped AgNPLs with a λ_{max} of 620 nm with rounded edges; no significant change in the LSPR of the AgNPLs was observed before irradiation (Figure 8B(a)). However, after 120 min of irradiation with the sodium lamp, the UV−vis spectra showed a significant decrease in the LSPR band of the AgNSs, an increase in the O.D., and a 60 nm red-shift in the LSPR band to λ_{max} of 680 nm (Figure 8B(b)). The appearance of the 680 nm band is characteristic of 40 nm AgNPLs with well-defined edges (Figure 1), which had an 85% conversion of rounded to sharper AgNPLs in the absence of exogenous Ag^+ ions and AgNP seeds.[51] Note that all citrate-

https://doi.org/10.1021/acs.jpcc.4c05948
J. Phys. Chem. C 2024, 128, 21784−21799

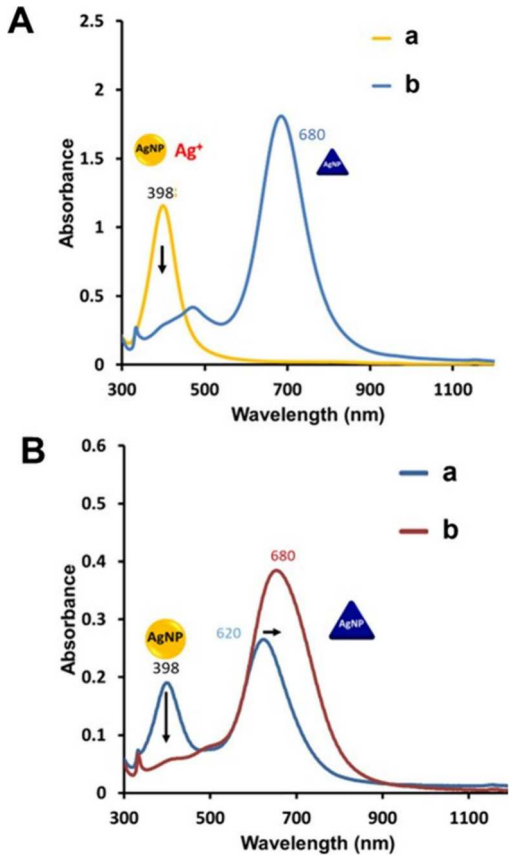

Figure 8. (A) Representative UV−vis spectra of 10 nm chemically synthesized citrate-capped AgNSs spiked with (a) 110 nM $AgNO_3$ before and (b) after light exposure for 2 h. (B) 40 nm purchased PVP-capped AgNPLs spiked with chemically synthesized 10 nm citrated-capped AgNSs (a) before and (b) after light exposure for 2 h.

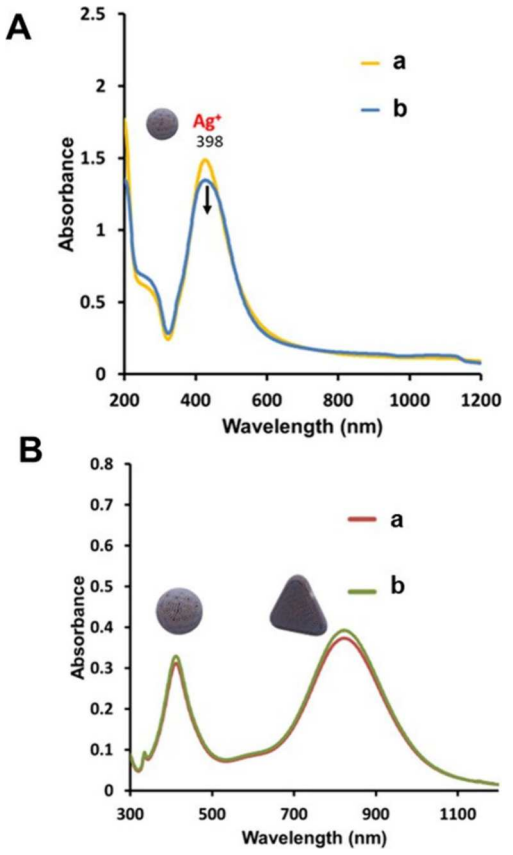

Figure 9. Representative UV−vis spectra of (A) unpurified 10 nm hybrid lipid-coated AgNSs with 322 mM citrate spiked with 110 nM $AgNO_3$ (a) before and (b) after light exposure for 2 h and (B) 40 nm hybrid lipid-coated AgNPLs spiked with 200 μL of 10 nm hybrid lipid-coated AgNSs (a) before and (b) after light exposure for 2 h.

capped AgNPs that undergo light irradiation with the sodium lamp convert to AgNPLs with well-defined edges at 75−85%.

Since no shape transformation is observed with unpurified hybrid lipid-coated AgNPs, which contain ∼64.4 mM of citrate per mL of nanoparticle from the reaction synthesis by $NaBH_4$ reduction, to determine if exogenous Ag^+ ions would induce an AgNP shape transformation similar to that observed in Figure 8, 110 nM of $AgNO_3$ was added to 10 nm hybrid lipid-coated AgNSs and exposed to light for 2 h. The UV−vis spectra show no shift in the LSPR band and a minimal 6.9% decrease in O.D., likely due to some loss of AgNSs (Figure 9A). Not surprisingly, when chemically synthesized 10 nm hybrid lipid-coated AgNSs are added to commercially purchased 70 nm hybrid lipid-coated AgNPLs, no change in the LSPR and O.D. is observed before and after light irradiation (Figure 9B). In the presence of exogenous Ag^+ ions and light, the hybrid lipid membrane architecture prevents shape transformation, indicating that it shields the nanoparticle from photooxidation caused by plasmon excitation. This shielding hinders the charge transfer process between adsorbates and the hot electrons (holes) generated from plasmon decay, which hinders nanoparticle growth and shape transformation.[30−32] Furthermore, this supports the conclusion that surface oxidation of AgNS seeds is necessary for Ag^+ production, AgNP growth, and shape transformation. Though the membrane architecture suppresses AgNP growth and shape transformation, it can "shape-lock" the AgNPs into place once synthesized to enhance their long-term stability and prevent Ag^+ ion release and degradation.[50−53,65] This design strategy improves long-term stability and homogeneity and enhances AgNP biocompatibility. More importantly, it is a new strategy for creating photostable AgNPs, which are needed for optical sensing, imaging, and drug delivery applications.

The Chemical Role of O_2 and Citrate on Photo-induced Shape Transformation. Previous studies have shown that O_2 is required to transform AgNSs to AgNPLs by oxidizing Ag^0 to Ag^+ ions.[44] Similarly, to evaluate the effect of O_2 on AgNS transformation to AgNPLs, 5 mL of chemically synthesized 10 nm citrate-capped AgNSs were assessed before and after light exposure in the presence of O_2 as well as after deoxygenation in the presence of light (Figure 10A). The UV−vis spectra of the citrate-capped AgNPs before light exposure in the presence of O_2 show a characteristic LSPR band at λ_{max} of 400 nm (Figure 10A(a)), which readily transforms to AgNPLs with a distinct band at 688 nm (Figure 10A(b)). However, upon deoxygenation with N_2, the UV−vis spectra show a broadening of the LSPR band, a 50% decrease in O.D., and no new LSPR band characteristically seen at 680 nm (Figure 10A(c)). This is consistent with literature reports that the absence of O_2 terminates Ag^+ ion generation by photooxidation, hindering growth and shape transformation. In addition, an increase in temperature can indirectly decrease O_2 and affect shape transformation. To evaluate the impact of exogenous Ag^+ ions on AgNP growth and transformation, 5 mL samples of 10 nm citrate-capped AgNSs with an O.D. of

https://doi.org/10.1021/acs.jpcc.4c05948
J. Phys. Chem. C 2024, 128, 21784−21799

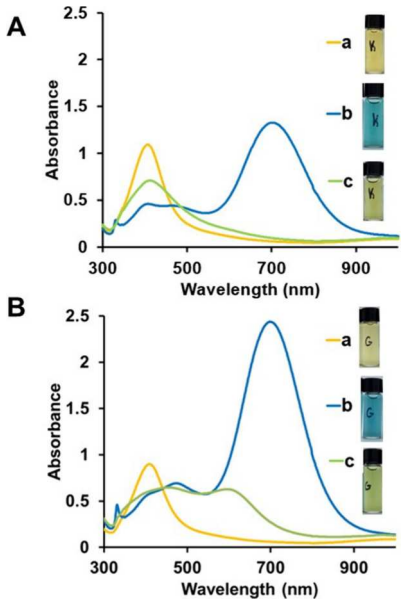

Figure 10. Representative UV−vis spectra of (A) 10 nm chemically synthesized citrate-capped AgNSs (a) before and (b) after 2 h of light exposure in the presence of O_2 (fwhm 94.4) and (c) after 2 h of light exposure in the presence of N_2 atmosphere and (B) 10 nm chemically synthesized citrate-capped AgNSs spiked with 110 mM $AgNO_3$ and (a) no light exposure in the presence of O_2, (b) after 2 h light exposure in the presence of O_2 (fwhm 87.8), and (c) after 2 h light exposure in the presence of a N_2 atmosphere.

1.12 were spiked with 110 nM of $AgNO_3$ and evaluated before light exposure, after light exposure in the presence of O_2, and after light exposure after deoxygenating with N_2. UV−vis spectra of the 10 nm citrate-capped AgNPs show no change in the O.D. or shift in the LSPR band upon spiking with $AgNO_3$ after 2 h of ambient light exposure in the presence of O_2 (Figure 10B(a)). However, upon exposure of this sample to the sodium lamp for 2 h, there is a characteristic decrease in the LSPR band at λ_{max} of 400 nm for AgNSs and a shift in the LSPR band to 697 nm that is similar to that of AgNPLs (Figure 10A(b)). Compared to the sample in Figure 10A(b) with no Ag^+ ions after light exposure, there is a 52.6% increase in O.D., and narrower full-width half max (fwhm) of 87.8 of the LSPR band in the presence of Ag^+ ions and O_2 compared to the fwhm of 94.4 observed in Figure 10B(b). Consistently, light exposure generates Ag^+ ions and, when coupled to exogenous Ag^+ ions, can transform to a higher concentration of AgNPLs in the presence of O_2. However, when the sample is deoxygenated with N_2 and exposed to light for 2 h, there is a decrease and shift in the LSPR band at λ_{max} of 400 to 454 nm for AgNSs, and a smaller new LSPR band appears at 601 nm, indicative of a new shape possibly smaller AgNPLs (Figure 10B(c)). This indicates that deoxygenation slows the photooxidation of AgNSs to generate a source of Ag^+ ions. In addition, since AgNSs are still observed, the LSPR band at 697 nm may be attributed to silver nanodisks, which have been shown to form upon adding exogenous Ag^+ ions in the presence of light (Figure 10B(c)).[36] These studies confirm that O_2 is necessary for AgNS oxidation and shape transformation[44,79] Moreover, adding a source of exogenous Ag^+ ions induces AgNP growth and shape transformation from the thermal reduction of Ag^+ ions by Ag^0NPs or by citrate that donates electrons upon plasmon excitation.[30−32]

Mirkin *et al.* suggested that nanoprisms are not formed without citrate or other oxygen-containing compounds such as tricarballylate, citramalate, and aconitate, and citrate is crucial for nanoprisms formation.[44,80−82] Citrate is a widely used thermal-reducing agent in preparing colloidal silver nanoparticles.[80−82] In this study, to confirm the role of trisodium citrate in shape transformation to AgNPLs, 5 mL of 10 nm citrate-capped AgNSs with an initial citrate concentration of 32.2 mM and an O.D. of 1.15 were placed under the sodium lamp for 2 h for conversion to AgNPLs. This sample and one not placed under the sodium lamp were rotovapped and resuspended in 0.5 mL of D_2O for ^1H NMR analysis with an estimated amount of trisodium citrate in the solution to be 322 mM. The ^1H NMR analysis of the AgNSs before light exposure shows a quadruplet at 2.57 ppm corresponding to the $-CH_3$ protons, showing an AB-type pattern of strongly coupled methylene proton resonances (Figure S5A). After light exposure for 2 h the quadruplet showed up at 2.46 ppm (Figure S5B). No signals that correspond to the two products that result from the thermal decomposition of citrate (d 2.47 ppm), 1, 3-acetone dicarboxylate with a proton signal at d 3.49 ppm and acetoacetate with proton signals at δ 3.41 and 2.25 pm.[44] In our studies, the maximum internal temperature of the solution from heating for 2 h was 98 °C, which is far below the temperature reported for the thermal decomposition of trisodium citrate at 325 °C.[83] Therefore, with this 70 W sodium lamp source within the time frame of our experiment, we did not see evidence of thermal decomposition of citrate. Therefore, citrate is not a reduction agent; the AgNPs act as electron donors upon plasmon excitation. This was confirmed in studies when 20 nm of commercially purchased citrate-capped AgNPs with an O.D. of 0.63 and minimal citrate on the surface showed no significant shape transformation under 2 h of light exposure (Figure S6A). Shape transformation is not observed because it has minimal citrate and no exogenous Ag^+ ions. Generation of Ag^+ ions by photooxidation is much slower with 20 nm than 10 nm AgNSs; hence, shape transformation is slower. Longer light exposure is required for transformation to occur. Adding 150 μL of 322 mM of citrate or 136 μL of 110 mM of $AgNO_3$ to the 20 nm citrate-capped AgNPs also showed no shape transformation upon photolysis (Figure S6B and C). The addition of trisodium citrate only showed a slight decrease of the O.D., while addition of exogenous Ag^+ ions resulted in 8.10% increase in O.D. that is likely due to AgNSs growth. The lack of shape transformation for the 20 nm AgNSs suggests that AgNPs that undergo rapid surface oxidation, such as smaller AgNSs or AgNPs with a more thermodynamically unstable facets are more likely to undergo shape transformation to more thermodynamically stable AgNPs.

Mechanism of AgNP Shape Transformation. These studies build on reported mechanisms by investigating other factors that play a role in photoinduced shape transformation. Similar to other studies, the photoinduced transformation of 10 nm citrate-capped AgNS seeds into AgNPLs is a multistep process. It first involves the oxidation of Ag^+ ions in the presence of light and O_2 and then the subsequent reduction of Ag^+ to Ag^0. The oxidation of 10 nm citrate-capped AgNSs to smaller AgNPs after photolysis is observed by TEM (Figure 1B and C), which surrounds AgNPLs with sharp edges or those that appear more rounded. Similar to other proposed mechanisms, reduction occurs from plasmon excitation by light on the AgNP surface to generate an electron−hole pair[6,23−28,44] since heating the solution to 98 °C without light

https://doi.org/10.1021/acs.jpcc.4c05948
J. Phys. Chem. C 2024, 128, 21784−21799

does not lead to shape transformation. Hot electrons are transferred to Ag^+ ions to generate Ag^0 near the [111]-facets on the AgNP surface for anisotropic growth of AgNPLs with 85% homogeneity. The transfer of electrons from AgNPs results in the photocatalytic generation of more Ag^+ ions in the presence of O_2 until there are no more seeds, which is evident in the UV−vis spectra by the loss of the LSPR band at λ_{max} at 400 nm. Light-induced plasmon excitation is required for shape transformation since the addition of exogenous $AgNO_3$ to 10 nm citrate-capped AgNSs does not induce shape transformation in the absence of light (Figure 2A), and the wavelength of light is an important parameter to increase the efficiency of homogeneous shape conversion (Figure 2B). That is, free Ag^+ ions are not enough for shape transformation. Some studies show that electron holes can be filled from the thermal reduction of citrate dissociated from the surface upon plasmon excitation to produce acetoacetate.[44,80−82] However, in this study, no evidence of thermal reduction of citrate was observed by ^1H NMR analysis (Figure S5) because the internal temperature of the solutions never reaches the high temperatures needed for thermal reduction with the lamp source used here. Instead, citrate is proposed to be a solubilizing agent for the Ag^+ ions since it is known to form complexes with Ag^+ ions at low concentrations. In other studies,[75,76] BSPP is proposed to solubilize the generated Ag^+ ions.[44] Similar to other studies, O_2 is required for photooxidation of AgNSs to Ag^+ ions if an exogenous Ag^+ ion source is unavailable (Figure 10). If O_2 is not present and no Ag^+ ions are available, no shape transformation occurs even in the presence of light (Figure 10A(c)). However, if a source of Ag^+ ions is present in the absence of O_2 and the presence of light, photoexcitation of the plasmon results in Ag^+ reduction to Ag^0, and shape conversion occurs (Figure 10B(c)). Based on the evidence presented here, the photooxidation/photoreduction process for converting 10 nm citrate-capped AgNSs to 40 nm AgNPLs occurs through an Ostwald ripening proposes and not coalescence (Scheme 1).

More interestingly, these studies show that chemically synthesized citrated-capped AgNPLs and AgNRs with a wide distribution of larger sizes and shapes (rounded AgNPLs (40 nm), AgNRs (44 nm), spheres (20 nm) and hexagons (22 nm)) undergo shape transformation upon plasmon excitation. The resulting citrated-capped AgNPLs with sharp edges had a 75% conversion efficiency with 15% 5 nm AgNSs and 10% 32 nm rounded AgNPLs remaining (Figure 3D and E). In comparison, the AgNRs had an 83% conversion efficiency to AgNPLs (40 nm) as the dominant nanoparticle type and 17% AgNSs (15 nm; Figure 4D and E). These studies show that the polydispersity of AgNPs can be improved with high efficiency and that shape conversion can happen with various shapes and AgNPs greater than 20 nm. This differs from earlier studies showing that AgNSs under 10 nm undergo shape transformation to form AgNPLs[30,44] or smaller nanoprisms grow to larger nanoprisms.[46] AgNPLs are the more thermodynamically favored shape since their size remains constant, and the distribution of other shapes is minimized significantly after photooxidation/photoreduction. In addition, since rounded AgNPLs are converted to AgNPLs with sharp edges, this mechanism involves photoablation of different sizes and shapes, followed by reduction of Ag^+ ions upon plasmonic excitation near the surface to undergo a photomorphic transition, consistent with other studies (Scheme 2).[84,85] During this transformation, less stable shapes such as rods, spheres, and hexagons are particularly prone to photoablation.

Scheme 1. Proposed Mechanism for Photomediated Pathway for AgNPLs from AgNS

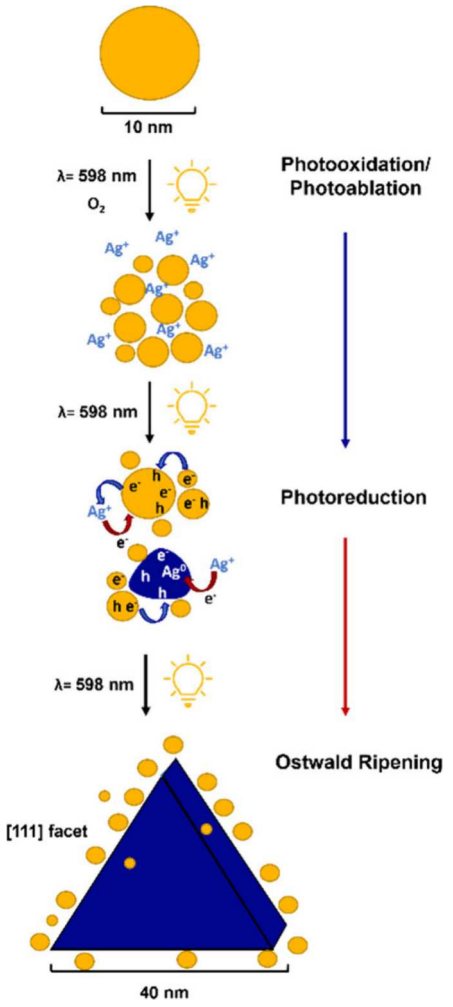

Scheme 2. Proposed Mechanism for Photomorphic Transformation of AgNPs to AgNPLs

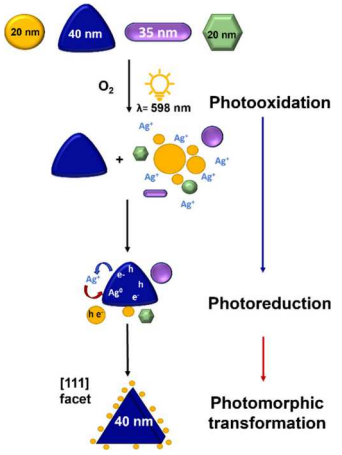

In this process, the nanoparticles dissolve into smaller Ag^+ ions under the influence of light.[86,87] These dissolved ions subsequently contribute to the anisotropic growth of AgNPLs, favoring their formation due to the lower surface energy associated with the [111] facet of these AgNPLs.[86] The photomorphic transformation thus aligns with the principle of

https://doi.org/10.1021/acs.jpcc.4c05948
J. Phys. Chem. C 2024, 128, 21784−21799

Table 1. Summary Table of the Reaction Parameters Tested and the Resulting Outcomes

Reaction Parameters	Outcome
Cit-AgNSs (10 nm) exposed to sodium lamp (598 nm)	10 nm → 3 nm (15%) + 40 nm (85%)
Shape conversion without light	No change
Shape conversion with heat (98℃)	No change
Cit-AgNSs (10 nm) exposed to LED (500 nm)	λ_{max} 401 nm → 456 nm, Mixed shape
Cit-AgNSs (10 nm) exposure to 420 nm Xenon	λ_{max} 401 nm → 563 nm, Mixed shape
598 nm sodium lamp on a mixture of Cit-capped AgNPLs, AgNSs, AgNRs and hexagon AgNPs	(50%) (40%) (10%) (1%) → (75%) + (15%) + (10%); (60%) (20%) (20%) → (83%) + (17%)
PVP-capping agent on shape transformation	(75%) + (25%)
Hybrid lipid coating on shape transformation	Photostable
PVP vs Cit vs hybrid lipid-coating on shape transformation	Hybrid lipid membrane > PVP > Cit
Exogenous Ag^+ effect on transformation	+ Ag^+
Exogenous AgNSs (10 nm) effect on PVP-AgNPLs transformation	+ (10 nm)
Exogenous Ag^+ effect on hybrid lipid-coated AgNS transformation	+ Ag^+
Inert N_2 atmosphere (no O_2) on shape transformation under 598 nm sodium lamp	+ N_2 → + Ag^+ Photooxidation and degradation
Exogenous Ag^+ and O_2 present together under sodium lamp	+ N_2 + Ag^+ → + Ag^+ + Small amount formed

minimizing the system's overall energy, where the triangular shape of the nanoplates represents a more stable configuration under the given photochemical conditions.[87,88] Additionally, the conversion efficiency is enhanced when the light source overlaps with the LSPR band of the nanoparticles, ensuring that the plasmonic effects are maximized, driving the process toward a high yield of uniform triangular nanoplates.[88]

Thus, far, the effect of surface coating on the rate of photooxidation/photoreduction and shape transformation provides the most valuable contribution to the current mechanistic understanding of photomediated shape transformation. Studies with PVP and a hybrid lipid-membrane architecture show the surface coating significantly impacts the photooxidation/photoreduction and shape transformation rate. Photomediated transformation of commercially purchased 100 nm PVP-capped AgNPLs, which contained 30% AgNPLs of 132 nm edge length and 50% rounded AgNPLs of 40 nm and 20% AgNSs of 20 nm, resulted in photoablation of the 132 nm AgNPLs to free Ag^+ ions and sharpening of the rounded 47.5 ± 11.6 nm AgNPLs (Figure 5). No change in the concentration of AgNSs is observed. This suggests that the 132 nm AgNPLs are the least thermodynamically favorable shape compared to AgNPLs and AgNSs. Furthermore, photoablation is followed by photomorphic change since the 47.5 ± 11.6 nm AgNPLs did not increase in size (Figure 5). This suggests that the PVP-coating protects the AgNSs and AgNPLs, and photooxidation is much slower in the presence of PVP and when the LSPR band does not overlap with the light source. This is also observed for PVP-capped AgNCs, which show minimal change in the UV−vis indicative of photoablation, photooxidation, and photoreduction (Figure 6). Compared to the PVP-coated AgNPLs, photodecomposition was even slower. When the AgNPs are coated with a hybrid lipid-coating designed to shield the AgNPs from the surface from oxidation, all AgNPs with this coating do not show any signs of surface oxidation, photooxidation/reduction, or shape transformation (Figure 7). That is, the hybrid lipid-coated AgNP plasmons are not excited by light, there is no excitation of electrons, and they are photostable.

Overall, AgNPs when coated withPVP or hybrid lipid membranes exhibit slow or resistance to shape transformation due to the protective barrier that inhibits both the oxidation and reduction processes, even in the presence of exogenous Ag^+ ions (Figure 9). This highlights the crucial role of surface chemistry in photomorphic transformation, where the absence of citrate or the presence of other stabilizing ligands can significantly alter the nanoparticle's susceptibility to shape conversion under light exposure.[89] Thus, the transformation into AgNPLs is a function of the initial shape and a delicate balance between the photophysical and photochemical environment surrounding the nanoparticles.

CONCLUSIONS

We have unequivocally demonstrated that photomediated shape transformation of AgNPs depends on the presence of a source of Ag^+ ions, an electron donor, and light. A summary of reaction conditions and the main outcomes of this study is highlighted in Table 1. The most convincing evidence comes from hybrid lipid-coated AgNPs that were found to be stable to light, oxidation, and reduction even in the presence of an oxidizing agent, a source of Ag^+ ions, a reducing agent, and plasmon excitation. Photolysis of 10 nm citrate-capped AgNSs with a sodium lamp source showed an 85% conversion of AgNSs to AgNPLs within 2 h, which depends on O_2 for oxidation of AgNSs and the wavelength of the light source. No shape transformation is observed in an inert atmosphere since no exogenous Ag^+ ions are present. However, under an inert atmosphere, if a source of Ag^+ ions is present, partial shape

https://doi.org/10.1021/acs.jpcc.4c05948
J. Phys. Chem. C 2024, 128, 21784−21799

transformation of AgNSs occurs when the plasmon is excited. In all cases, AgNSs or other AgNP shapes become electron donors upon plasmon excitation to form electron−hole pairs on the surface to reduce Ag^+ ions to Ag^0, demonstrating light is a critical parameter for this process. Under the conditions of this study, the AgNPs are electron donors and not citrate, as no thermal reduction products of citrate are observed since the reaction temperature is below 100 °C. This study also showed that shape transformation is not isolated to 10 nm AgNSs. AgNPs larger than 10 nm, comprised of AgNSs, hexagons, AgNRs, and rounded AgNPLs, can undergo shape transformation. However, the surface coating on the AgNP significantly impacts the shape transformation rate and the resulting AgNPs' homogeneity. The AgNPs coated with citrate exhibited a considerably higher conversion efficiency to AgNPLs, which is markedly slower in the presence of PVP coating. Interestingly, it was observed that PVP-coated AgNPLs with more edges underwent surface oxidation more readily than PVP-AgNCs. Notably, there was no photo-oxidation/reduction with the hybrid lipid-coated AgNPs of any size or shape, demonstrating plasmon excitation and formation of electron−hole pairs on the surface are hindered by the hybrid lipid-coating. The hybrid lipid-coating effectively shields the AgNP surface from access to Ag^+ ions, preventing shape growth and transformation and maintaining their photostability.

This study emphasizes the crucial role of light wavelength in fine-tuning the physical and chemical properties and the homogeneity of AgNPs. Harnessing the power of light, we can transform heterogeneous materials from chemical processes into highly homogeneous nanomaterial batches, which is essential for cutting-edge applications in imaging, drug delivery, and research into nanomaterial toxicity and interactions with biological systems. Furthermore, the study further highlights the high potential of utilizing light to precisely control the size and shape at the nanoscale level by manipulating the illumination conditions. This opens up exciting possibilities for using light wavelengths and photon flux to craft uniform nanomaterial samples, extending beyond AgNPLs to encompass AgNRs or AgNCs of diverse sizes. Additionally, the study sheds light on how light-induced degradation of AgNPs and hybrid lipid membranes offers a versatile strategy for stabilizing materials of any shape or size. This minimizes alterations to their physical and chemical properties, thereby preserving their optoelectronic properties critical for advanced applications such as optical and X-ray imaging. This work complements the growing body of work on the fundamental processes underlying nanoparticle growth, shape transformation, and approaches to increasing photostable homogeneous nanomaterials.

■ ASSOCIATED CONTENT

Supporting Information

The Supporting Information is available free of charge at https://pubs.acs.org/doi/10.1021/acs.jpcc.4c05948.

Sodium lamp setup (Figure S1); quantities of materials needed for hybrid lipid-coated nanomaterials synthesis for AgNRs, AgNCs, and AgNSs (Table S1); representative UV−vis spectra of the hybrid lipid-coated AgNPs after cyanide etching (Figure S2); representative TEM images indicating how nanoparticles were measured (Figure S3); UV−vis spectra of citrate-capped AgNSs before and after light exposure with a 150-W lamp (Figure S4); ^{1}H NMR spectroscopy of citrate-capped-AgNSs and citrate-capped AgNPLs after light exposure (Figure S5); representative UV−vis spectra of 20 nm citrate-capped AgNSs in excess $AgNO_3$ and trisodium citrate (Figure S6); representative histograms of all silver nanoparticles examined (Figure S7) (PDF).

■ AUTHOR INFORMATION

Corresponding Author

Marilyn R. Mackiewicz − *Department of Chemistry, Oregon State University, Corvallis, Oregon 97331, United States;* orcid.org/0000-0002-5669-8714; Email: marilyn.mackiewicz@oregonstate.edu

Authors

Citlali Nieves Lira − *Department of Chemistry, Oregon State University, Corvallis, Oregon 97331, United States*

Hao Yue − *Department of Chemistry, Oregon State University, Corvallis, Oregon 97331, United States*

Complete contact information is available at: https://pubs.acs.org/10.1021/acs.jpcc.4c05948

Notes

The authors declare no competing financial interest.

■ ACKNOWLEDGMENTS

We want to acknowledge the National Science Foundation Career Award support under grant 2145427.

■ ABBREVIATIONS

AgNPs, silver nanoparticles; PC, phosphatidylcholine; SOA, sodium oleate; HT, hexanethiol; AgNSs, silver nanospheres; AgNPLs, silver triangular nanoplates; AgNCs, silver nanocubes; AgNRs, silver nanorods; TEM, transmission electron microscopy; NMR, nuclear magnetic resonance

■ REFERENCES

(1) Kowsalya, E.; MosaChristas, K.; Balashanmugam, P.; Manivasagan, V.; Devasena, T.; Jaquline, C. R. I. Sustainable use of biowaste for synthesis of silver nanoparticles and its incorporation into gelatin-based nanocomposite films for antimicrobial food packaging applications. *Journal of Food Process Engineering* **2021**, *44* (3), No. e13641.

(2) Istiqola, A.; Syafiuddin, A. A review of silver nanoparticles in food packaging technologies: Regulation, methods, properties, migration, and future challenges. *Journal of the Chinese Chemical Society* **2020**, *67* (11), 1942−1956.

(3) Feng, Q. L.; Wu, J.; Chen, G. Q.; Cui, F. Z.; Kim, T. N.; Kim, J. O. A mechanistic study of the antibacterial effect of silver ions on Escherichia coli and Staphylococcus aureus. *J. Biomed. Mater. Res.* **2000**, *52* (4), 662−668.

(4) Zhou, S.; Li, J.; Gilroy, K. D.; Tao, J.; Zhu, C.; Yang, X.; Sun, X.; Xia, Y. Facile Synthesis of Silver Nanocubes with Sharp Corners and Edges in an Aqueous Solution. *ACS Nano* **2016**, *10* (11), 9861−9870.

(5) Liang, H.; Wang, W.; Huang, Y.; Zhang, S.; Wei, H.; Xu, H. Controlled Synthesis of Uniform Silver Nanospheres. *J. Phys. Chem. C* **2010**, *114* (16), 7427−7431.

(6) D'Agostino, A.; Taglietti, A.; Grisoli, P.; Dacarro, G.; Cucca, L.; Patrini, M.; Pallavicini, P. Seed mediated growth of silver nanoplates on glass: exploiting the bimodal antibacterial effect by near IR photothermal action and Ag+ release. *RSC Adv.* **2016**, *6* (74), 70414−70423.

(7) Kim, Y.-K.; Min, D.-H. Surface confined successive growth of silver nanoplates on a solid substrate with tunable surface plasmon resonance. *RSC Adv.* **2014**, *4* (14), 6950−6956.
(8) Xu, H.; Hao, S.; Wiley, B. J. Anisotropic Growth of Silver Nanocubes: The Role of Bromide Adsorption and Hydrophilic Polymers. *Chem. Mater.* **2023**, *35* (17), 7196−7207.
(9) Shin, S. W.; Song, I. H.; Um, S. H. Role of physicochemical properties in nanoparticle toxicity. *Nanomaterials* **2015**, *5* (3), 1351−1365.
(10) Rezić, I., Nanoparticles for Biomedical Application and Their Synthesis. *Polymers* **2022**, *14* (22).4961
(11) Adewale, O. B.; Davids, H.; Cairncross, L.; Roux, S. Toxicological Behavior of Gold Nanoparticles on Various Models: Influence of Physicochemical Properties and Other Factors. *International Journal of Toxicology* **2019**, *38* (5), 357−384.
(12) Augustine, R.; Hasan, A.; Primavera, R.; Wilson, R. J.; Thakor, A. S.; Kevadiya, B. D. Cellular uptake and retention of nanoparticles: Insights on particle properties and interaction with cellular components. *Materials Today Communications* **2020**, *25*, No. 101692.
(13) Yagublu, V.; Karimova, A.; Hajibabazadeh, J.; Reissfelder, C.; Muradov, M.; Bellucci, S.; Allahverdiyev, A. Overview of Physicochemical Properties of Nanoparticles as Drug Carriers for Targeted Cancer Therapy. *Journal of Functional Biomaterials* **2022**, *13* (4), 196.
(14) Sabourian, P.; Yazdani, G.; Ashraf, S. S.; Frounchi, M.; Mashayekhan, S.; Kiani, S.; Kakkar, A. Effect of Physico-Chemical Properties of Nanoparticles on Their Intracellular Uptake. *International journal of molecular sciences* **2020**, *21* (21), 8019.
(15) Yaqoob, A. A.; Umar, K.; Ibrahim, M. N. M. Silver nanoparticles: various methods of synthesis, size affecting factors and their potential applications−a review. *Applied Nanoscience* **2020**, *10* (5), 1369−1378.
(16) Zhang, J.; Langille, M. R.; Mirkin, C. A. Synthesis of Silver Nanorods by Low Energy Excitation of Spherical Plasmonic Seeds. *Nano Lett.* **2011**, *11* (6), 2495−2498.
(17) Salem, J. K.; Draz, M. A. Synthesis and application of silver nanorods for the colorimetric detection of sulfate in water. *Inorg. Chem. Commun.* **2020**, *116*, No. 107900.
(18) Jana, N. R.; Gearheart, L.; Murphy, C. J. Wet chemical synthesis of silver nanorods and nanowires of controllable aspect ratio. *Chem. Commun.* **2001**, No. 7, 617−618.
(19) Ojha, A. K.; Forster, S.; Kumar, S.; Vats, S.; Negi, S.; Fischer, I. Synthesis of well−dispersed silver nanorods of different aspect ratios and their antimicrobial properties against gram positive and negative bacterial strains. *J. Nanobiotechnol.* **2013**, *11* (1), 42.
(20) Pawlik, V.; Zhou, S.; Zhou, S.; Qin, D.; Xia, Y. Silver Nanocubes: From Serendipity to Mechanistic Understanding, Rational Synthesis, and Niche Applications. *Chem. Mater.* **2023**, *35* (9), 3427−3449.
(21) Gheitaran, R.; Afkhami, A.; Madrakian, T. Effect of light at different wavelengths on polyol synthesis of silver nanocubes. *Sci. Rep* **2022**, *12* (1), No. 19202.
(22) Zhang, D.; Chen, Y.; Huang, Y. S.; Huang, Q.; Kwan Li, K.; Xia, Y. Robust, Reproducible, and Scalable Synthesis of Silver Nanocubes. *Chemistry−A European Journal* **2024**, *30*, No. e202400833.
(23) Lai, Y.-C.; Wang, Y.-C.; Chiu, Y.-C.; Liao, Y.-C. Microwave-Assisted Synthesis for Silver Nanoplates with a High Aspect Ratio. *Langmuir* **2021**, *37* (46), 13689−13695.
(24) Zhang, Z.; Xue, T.; Qin, M.; Wang, Y.; Shi, Q.; Wang, L.; Zhao, Y.; Yang, Z. Solvothermal Preparation of Crystal Seeds and Anisotropy-Controlled Growth of Silver Nanoplates. *ACS Omega* **2024**, *9* (26), 28659−28665.
(25) Zhang, J.; Langille, M. R.; Mirkin, C. A. Photomediated synthesis of silver triangular bipyramids and prisms: the effect of pH and BSPP. *J. Am. Chem. Soc.* **2010**, *132* (35), 12502−12510.
(26) Tang, B.; Xu, S.; An, J.; Zhao, B.; Xu, W. Photoinduced Shape Conversion and Reconstruction of Silver Nanoprisms. *J. Phys. Chem. C* **2009**, *113* (17), 7025−7030.
(27) Haber, J.; Sokolov, K. Synthesis of stable citrate-capped silver nanoprisms. *Langmuir* **2017**, *33* (40), 10525−10530.
(28) Verma, S.; Rao, B. T.; Srivastava, A.; Srivastava, D.; Kaul, R.; Singh, B. A facile synthesis of broad plasmon wavelength tunable silver nanoparticles in citrate aqueous solutions by laser ablation and light irradiation. *Colloids Surf., A* **2017**, *527*, 23−33.
(29) Kim, B.-H.; Lee, J.-S. One-pot photochemical synthesis of silver nanodisks using a conventional metal-halide lamp. *Mater. Chem. Phys.* **2015**, *149*, 678−685.
(30) Chen, S.; Carroll, D. L. Synthesis and Characterization of Truncated Triangular Silver Nanoplates. *Nano Lett.* **2002**, *2* (9), 1003−1007.
(31) Kaabipour, S.; Hemmati, S. A review on the green and sustainable synthesis of silver nanoparticles and one-dimensional silver nanostructures. *Beilstein Journal of Nanotechnology* **2021**, *12*, 102−136.
(32) Wang, H.; Qiao, X.; Chen, J.; Ding, S. Preparation of silver nanoparticles by chemical reduction method. *Colloids Surf., A* **2005**, *256* (2), 111−115.
(33) Zhong, Y.; Liang, G.; Jin, W.; Jian, Z.; Wu, Z.; Chen, Q.; Cai, Y.; Zhang, W. Preparation of triangular silver nanoplates by silver seeds capped with citrate-CTA+. *RSC Adv.* **2018**, *8* (51), 28934−28943.
(34) Tang, B.; Sun, L.; Li, J.; Zhang, M.; Wang, X. Sunlight-driven synthesis of anisotropic silver nanoparticles. *Chemical Engineering Journal* **2015**, *260*, 99−106.
(35) Zhang, Q.; Yin, Y. Beyond spheres: Murphy's silver nanorods and nanowires. *Chem. Commun.* **2013**, *49* (3), 215−217.
(36) Maillard, M.; Huang, P.; Brus, L. Silver Nanodisk Growth by Surface Plasmon Enhanced Photoreduction of Adsorbed [Ag+]. *Nano Lett.* **2003**, *3* (11), 1611−1615.
(37) Jara, N.; Milán, N. S.; Rahman, A.; Mouheb, L.; Boffito, D. C.; Jeffryes, C.; Dahoumane, S. A. Photochemical Synthesis of Gold and Silver Nanoparticles—A Review. *Molecules* **2021**, *26* (15), 4585.
(38) Ciou, S.-H.; Cao, Y.-W.; Huang, H.-C.; Su, D.-Y.; Huang, C.-L. SERS Enhancement Factors Studies of Silver Nanoprism and Spherical Nanoparticle Colloids in The Presence of Bromide Ions. *J. Phys. Chem. C* **2009**, *113* (22), 9520−9525.
(39) Zheng, X.; Peng, Y.; Lombardi, J. R.; Cui, X.; Zheng, W. Photochemical growth of silver nanoparticles with mixed-light irradiation. *Colloid Polym. Sci.* **2016**, *294* (5), 911−916.
(40) Yang, L.-C.; Lai, Y.-S.; Tsai, C.-M.; Kong, Y.-T.; Lee, C.-I.; Huang, C.-L. One-Pot Synthesis of Monodispersed Silver Nanodecahedra with Optimal SERS Activities Using Seedless Photo-Assisted Citrate Reduction Method. *J. Phys. Chem. C* **2012**, *116* (45), 24292−24300.
(41) Tuan Anh, M. N.; Nguyen, D. T. D.; Ke Thanh, N. V.; Phuong Phong, N. T.; Nguyen, D. H.; Nguyen-Le, M.-T. Photochemical synthesis of silver nanodecahedrons under blue LED irradiation and their SERS activity. *Processes* **2020**, *8* (3), 292.
(42) Remziye, G.; Gülbahar, E., Synthesis of Silver Nanoparticles. In *Silver Nanoparticles*; Khan, M., Ed.; IntechOpen: Rijeka, 2018; chapter 1.
(43) Yu, P.; Huang, J.; Tang, J. Observation of Coalescence Process of Silver Nanospheres During Shape Transformation to Nanoprisms. *Nanoscale Res. Lett.* **2011**, *6* (1), 46.
(44) Xue, C.; Métraux, G. S.; Millstone, J. E.; Mirkin, C. A. Mechanistic Study of Photomediated Triangular Silver Nanoprism Growth. *J. Am. Chem. Soc.* **2008**, *130* (26), 8337−8344.
(45) Jin, R.; Cao, Y.; Mirkin, C. A.; Kelly, K. L.; Schatz, G. C.; Zheng, J. G. Photoinduced Conversion of Silver Nanospheres to Nanoprisms. *Science* **2001**, *294* (5548), 1901−1903.
(46) Lee, G. P.; Shi, Y.; Lavoie, E.; Daeneke, T.; Reineck, P.; Cappel, U. B.; Huang, D. M.; Bach, U. Light-Driven Transformation Processes of Anisotropic Silver Nanoparticles. *ACS Nano* **2013**, *7* (7), 5911−5921.
(47) Jin, R.; Charles Cao, Y.; Hao, E.; Métraux, G. S.; Schatz, G. C.; Mirkin, C. A. Controlling anisotropic nanoparticle growth through plasmon excitation. *Nature* **2003**, *425* (6957), 487−490.

https://doi.org/10.1021/acs.jpcc.4c05948
J. Phys. Chem. C 2024, 128, 21784−21799

(48) Watanabe, K.; Menzel, D.; Nilius, N.; Freund, H.-J. Photochemistry on Metal Nanoparticles. *Chem. Rev.* **2006**, *106* (10), 4301−4320.
(49) Huang, T.; Xu, X.-H. N. Synthesis and Characterization of Tunable Rainbow Colored Colloidal Silver Nanoparticles Using Single-Nanoparticle Plasmonic Microscopy and Spectroscopy. *J. Mater. Chem.* **2010**, *20* (44), 9867−9876.
(50) Miesen, T. J.; Engstrom, A. M.; Frost, D. C.; Ajjarapu, R.; Ajjarapu, R.; Lira, C. N.; Mackiewicz, M. R. A hybrid lipid membrane coating "shape-locks" silver nanoparticles to prevent surface oxidation and silver ion dissolution. *RSC Adv.* **2020**, *10* (27), 15677−15693.
(51) Nieves Lira, C.; Carpenter, A. P.; Baio, J. E.; Harper, B. J.; Harper, S. L.; Mackiewicz, M. R. Size- and Shape-Dependent Interactions of Lipid-Coated Silver Nanoparticles: An Improved Mechanistic Understanding through Model Cell Membranes and In Vivo Toxicity. *Chem. Res. Toxicol.* **2024**, *37* (6), 968−980.
(52) Harper, B. J.; Engstrom, A. M.; Harper, S. L.; Mackiewicz, M. R. Impacts of Differentially Shaped Silver Nanoparticles with Increasingly Complex Hydrophobic Thiol Surface Coatings in Small-Scale Laboratory Microcosms. *Nanomaterials* **2024**, *14* (8), 654.
(53) Cunningham, B.; Engstrom, A. M.; Harper, B. J.; Harper, S. L.; Mackiewicz, M. R. Silver Nanoparticles Stable to Oxidation and Silver Ion Release Show Size-Dependent Toxicity In Vivo. *Nanomaterials (Basel, Switzerland)* **2021**, *11* (6), 1516.
(54) Cunningham, B.; Engstrom, A. M.; Harper, B. J.; Harper, S. L.; Mackiewicz, M. R. Silver Nanoparticles Stable to Oxidation and Silver Ion Release Show Size-Dependent Toxicity In Vivo. *Nanomaterials* **2021**, *11* (6), 1516.
(55) Garcia, P. R. A. F.; Prymak, O.; Grasmik, V.; Pappert, K.; Wlysses, W.; Otubo, L.; Epple, M.; Oliveira, C. L. P. An in situ SAXS investigation of the formation of silver nanoparticles and bimetallic silver−gold nanoparticles in controlled wet-chemical reduction synthesis. *Nanoscale Advances* **2020**, *2* (1), 225−238.
(56) Knaapila, M.; Vainio, U.; Canton, S. E.; Karlsson, G. Structural Study of the Photo-Mediated Growth of Silver Nanoprisms. *Molecules* **2020**, *25* (22), 5413.
(57) Link, S.; El-Sayed, M. A. Shape and size dependence of radiative, non-radiative and photothermal properties of gold nanocrystals. *Int. Rev. Phys. Chem.* **2000**, *19* (3), 409−453.
(58) Mai Ngoc, T. A.; Nguyen, D. T. D.; Ngo, V. K. T.; Nguyen Thi, P. P.; Nguyen, D. H.; Nguyen-Le, M.-T. A Systematic Study of the One-Pot Fabrication of Anisotropic Silver Nanoplates with Controllable Size and Shape for SERS Amplification. *Plasmonics* **2020**, *15* (6), 2185−2194.
(59) Biswas, S.; Kole, A. K.; Sarkar, R.; Kumbhakar, P. Synthesis of anisotropic nanostructures of silver for its possible applications in glucose and temperature sensing. *Materials Research Express* **2014**, *1* (4), No. 045043.
(60) Kamat, P. V.; Flumiani, M.; Hartland, G. V. Picosecond Dynamics of Silver Nanoclusters. Photoejection of Electrons and Fragmentation. *J. Phys. Chem. B* **1998**, *102* (17), 3123−3128.
(61) Gorka, D. E.; Osterberg, J. S.; Gwin, C. A.; Colman, B. P.; Meyer, J. N.; Bernhardt, E. S.; Gunsch, C. K.; DiGulio, R. T.; Liu, J. Reducing Environmental Toxicity of Silver Nanoparticles through Shape Control. *Environ. Sci. Technol.* **2015**, *49* (16), 10093−8.
(62) Stevenson, A. P.; Blanco Bea, D.; Civit, S.; Antoranz Contera, S.; Iglesias Cerveto, A.; Trigueros, S. Three strategies to stabilise nearly monodispersed silver nanoparticles in aqueous solution. *Nanoscale Res. Lett.* **2012**, *7* (1), 151.
(63) Sanedrin, R. G.; Huang, L.; Jang, J. W.; Kakkassery, J.; Mirkin, C. A. Polyethylene glycol as a novel resist and sacrificial material for generating positive and negative nanostructures. *Small* **2008**, *4* (7), 920−4.
(64) Shkilnyy, A.; Soucé, M.; Dubois, P.; Warmont, F.; Saboungi, M.-L.; Chourpa, I. Poly(ethylene glycol)-stabilized silver nanoparticles for bioanalytical applications of SERS spectroscopy. *Analyst* **2009**, *134* (9), 1868−1872.
(65) Engstrom, A. M.; Wu, H.; Mackiewicz, M. R.; Harper, S. L. Controlling Silver Ion Release of Silver Nanoparticles with Hybrid Lipid Membranes with Long-Chain Hydrophobic Thiol Anchors Decreases in Vivo Toxicity. *International Journal of Engineering Research and Applications* **2020**, *10* (9), 12−28.
(66) Templeton, A. C.; Hostetler, M. J.; Kraft, C. T.; Murray, R. W. Reactivity of Monolayer-Protected Gold Cluster Molecules: Steric Effects. *J. Am. Chem. Soc.* **1998**, *120* (8), 1906−1911.
(67) Hajizadeh, S.; Farhadi, K.; Forough, M.; Sabzi, R. E. Silver nanoparticles as a cyanide colorimetric sensor in aqueous media. *Analytical Methods* **2011**, *3* (11), 2599−2603.
(68) Sitaula, S.; Mackiewicz, M. R.; Reed, S. M. Gold nanoparticles become stable to cyanide etch when coated with hybrid lipid bilayers. *Chem. Commun.* **2008**, No. 26, 3013−3015.
(69) Mackiewicz, M. R.; Ayres, B. R.; Reed, S. M. Reversible, reagentless solubility changes in phosphatidylcholine-stabilized gold nanoparticles. *Nanotechnology* **2008**, *19* (11), No. 115607.
(70) Hamilton, D. J.; Cai, Y.; Kaur, R.; Marquart, G. W.; Mackiewicz, M. R.; Reed, S. M. *Lipid-Coated Gold Nanoparticles as Probes for Membrane Binding*; Humana Press: Totowa, NJ, pp 1−16.
(71) Engstrom, A. M.; Faase, R. A.; Marquart, G. W.; Baio, J. E.; Mackiewicz, M. R.; Harper, S. L. Size-Dependent Interactions of Lipid-Coated Gold Nanoparticles: Developing a Better Mechanistic Understanding Through Model Cell Membranes and in vivo Toxicity. *International journal of nanomedicine* **2020**, *15*, 4091−4104.
(72) Germain, V.; Li, J.; Ingert, D.; Wang, Z. L.; Pileni, M. P. Stacking Faults in Formation of Silver Nanodisks. *J. Phys. Chem. B* **2003**, *107* (34), 8717−8720.
(73) Salzemann, C.; Urban, J.; Lisiecki, I.; Pileni, M.-P. Characterization and Growth Process of Copper Nanodisks. *Adv. Funct. Mater.* **2005**, *15* (8), 1277−1284.
(74) Fan, F.-R.; Ding, Y.; Liu, D.-Y.; Tian, Z.-Q.; Wang, Z. L. Facet-Selective Epitaxial Growth of Heterogeneous Nanostructures of Semiconductor and Metal: ZnO Nanorods on Ag Nanocrystals. *J. Am. Chem. Soc.* **2009**, *131* (34), 12036−12037.
(75) Lu, Y.; Zhang, C.; Hao, R.; Zhang, D.; Fu, Y.; Moeendarbari, S.; Pickering, C. S.; Hao, Y.; Liu, Y. Morphological transformations of silver nanoparticles in seedless photochemical synthesis. *Materials Research Express* **2016**, *3* (5), No. 055014.
(76) Jain, P. K.; Qian, W.; El-Sayed, M. A. Ultrafast Cooling of Photoexcited Electrons in Gold Nanoparticle−Thiolated DNA Conjugates Involves the Dissociation of the Gold−Thiol Bond. *J. Am. Chem. Soc.* **2006**, *128* (7), 2426−2433.
(77) Richardson, H. H.; Hickman, Z. N.; Govorov, A. O.; Thomas, A. C.; Zhang, W.; Kordesch, M. E. Thermooptical Properties of Gold Nanoparticles Embedded in Ice: Characterization of Heat Generation and Melting. *Nano Lett.* **2006**, *6* (4), 783−788.
(78) Govorov, A. O.; Richardson, H. H. Generating heat with metal nanoparticles. *Nano Today* **2007**, *2* (1), 30−38.
(79) Wojtysiak, S.; Kudelski, A. Influence of oxygen on the process of formation of silver nanoparticles during citrate/borohydride synthesis of silver sols. *Colloids Surf., A* **2012**, *410*, 45−51.
(80) Lee, P. C.; Meisel, D. Adsorption and surface-enhanced Raman of dyes on silver and gold sols. *J. Phys. Chem.* **1982**, *86* (17), 3391−3395.
(81) Munro, C. H.; Smith, W. E.; Garner, M.; Clarkson, J.; White, P. C. Characterization of the Surface of a Citrate-Reduced Colloid Optimized for Use as a Substrate for Surface-Enhanced Resonance Raman Scattering. *Langmuir* **1995**, *11* (10), 3712−3720.
(82) La Spina, R.; Mehn, D.; Fumagalli, F.; Holland, M.; Reniero, F.; Rossi, F.; Gilliland, D. Synthesis of Citrate-Stabilized Silver Nanoparticles Modified by Thermal and pH Preconditioned Tannic Acid. *Nanomaterials (Basel, Switzerland)* **2020**, *10* (10), 2031.
(83) Gao, J.; Wang, Y.; Hao, H. Investigations on dehydration processes of trisodium citrate hydrates. *Frontiers of Chemical Science and Engineering* **2012**, *6* (3), 276−281.
(84) Lee, G. P.; Bignell, L. J.; Romeo, T. C.; Razal, J. M.; Shepherd, R. L.; Chen, J.; Minett, A. I.; Innis, P. C.; Wallace, G. G. The citrate-mediated shape evolution of transforming photomorphic silver nanoparticles. *Chem. Commun.* **2010**, *46* (41), 7807−7809.

https://doi.org/10.1021/acs.jpcc.4c05948
J. Phys. Chem. C 2024, 128, 21784−21799

(85) Phetsahai, A.; Eiamchai, P.; Thamaphat, K.; Limsuwan, P. The Morphological Evolution of Self-Assembled Silver Nanoparticles under Photoirradiation and Their SERS Performance. *Processes* **2023**, *11* (7), 2207.
(86) Jin, R.; Cao, Y.; Mirkin, C. A.; Kelly, K. L.; Schatz, G. C.; Zheng, J. G. Photoinduced conversion of silver nanospheres to nanoprisms. *Science* **2001**, *294* (5548), 1901−3.
(87) Halas, N. J.; Lal, S.; Chang, W.-S.; Link, S.; Nordlander, P. Plasmons in Strongly Coupled Metallic Nanostructures. *Chem. Rev.* **2011**, *111* (6), 3913−3961.
(88) Zhang, Q.; Li, W.; Moran, C.; Zeng, J.; Chen, J.; Wen, L. P.; Xia, Y. Seed-mediated synthesis of Ag nanocubes with controllable edge lengths in the range of 30−200 nm and comparison of their optical properties. *J. Am. Chem. Soc.* **2010**, *132* (32), 11372−8.
(89) Murphy, C. J.; Sau, T. K.; Gole, A. M.; Orendorff, C. J.; Gao, J.; Gou, L.; Hunyadi, S. E.; Li, T. Anisotropic Metal Nanoparticles: Synthesis, Assembly, and Optical Applications. *J. Phys. Chem. B* **2005**, *109* (29), 13857−13870.

https://doi.org/10.1021/acs.jpcc.4c05948
J. Phys. Chem. C 2024, 128, 21784−21799